Exploring different virulent proteins of human respiratory syncytial virus for designing a novel epitope-based polyvalent vaccine: Immunoinformatics and molecular dynamics approaches

Abu Tayab Moin[1,¶], Md. Asad Ullah[2,¶], Rajesh B. Patil[3], Nairita Ahsan Faruqui[4], Bishajit Sarkar[2], Yusha Araf[5], Sowmen Das[6], Khaza Md. Kapil Uddin[1], Md Shakhawat Hossain[1], Md. Faruque Miah[5], Mohammad Ali Moni[7, 8], Dil Umme Salma Chowdhury[1*], Saiful Islam[9*]

[1]Department of Genetic Engineering and Biotechnology, Faculty of Biological Sciences, University of Chittagong, Chattogram, Bangladesh

[2]Department of Biotechnology and Genetic Engineering, Faculty of Biological Sciences, Jahangirnagar University, Savar, Dhaka, Bangladesh

[3]Sinhgad Technical Education Society's, Sinhgad College of Pharmacy, Department of Pharmaceutical Chemistry, Maharashtra, India

[4]Biotechnology Program, Department of Mathematics and Natural Sciences, School of Data and Sciences, BRAC University, Dhaka, Bangladesh

[5]Department of Genetic Engineering and Biotechnology, School of Life Sciences, Shahjalal University of Science and Technology, Sylhet, Bangladesh

[6]Department of Computer Science and Engineering, School of Physical Sciences, Shahjalal University of Science and Technology, Sylhet, Bangladesh

[7]Bone Biology Division, The Garvan Institute of Medical Research, Darlinghurst, NSW Sydney, Australia

[8]WHO Collaborating Centre on eHealth, UNSW Digital Health, School of Public Health and Community Medicine, Faculty of Medicine, UNSW Sydney, Australia

[9]Bangladesh Council of Scientific and Industrial Research (BCSIR), Chattogram Laboratories, Chattogram, Bangladesh

¶These authors contributed equally to this work

*Corresponding author:

Dil Umme Salma Chowdhury (dilgeb@cu.ac.bd), &

Saiful Islam (saifbiology80@gmail.com)

Abstract

Human Respiratory Syncytial Virus (RSV) is one of the most prominent causes of lower respiratory tract infections (LRTI), contributory to infecting people from all age groups - a majority of which comprises infants and children. The implicated severe RSV infections lead to numerous deaths of multitudes of the overall population, predominantly the children, every year. Consequently, despite several distinctive efforts to develop a vaccine against the RSV as a potential countermeasure, there is no approved or licensed vaccine available yet, to control the RSV infection effectively. Therefore, through the utilization of immunoinformatics tools, a computational approach was taken in this study, to design and construct a multi-epitope polyvalent vaccine against the RSV-A and RSV-B strains of the virus. Potential predictions of the T-cell and B-cell epitopes were followed by extensive tests of antigenicity, allergenicity, toxicity, conservancy, homology to human proteome, transmembrane topology, and cytokine-inducing ability. The most promising epitopes (i.e. 13 CTL epitopes, 9 HTL epitopes, and 10 LBL epitopes) exhibiting full conservancy were then selected for designing the peptide fusion with appropriate linkers, having hBD-3 as the adjuvant. The peptide vaccine was modeled, refined, and validated to further improve the structural attributes. Following this, molecular docking analysis with specific TLRs was carried out which revealed excellent interactions and global binding energies. Additionally, molecular dynamics (MD) simulation was conducted which ensured the stability of the interactions between vaccine and TLR. Furthermore, mechanistic approaches to imitate and predict the potential immune response generated by the administration of vaccines were determined through immune simulations. Owing to an overall evaluation, *in silico* cloning was carried out in efforts to generate recombinant pETite plasmid vectors for subsequent mass production of the vaccine peptide, incorporated within *E.coli*. However, more in vitro and in vivo experiments can further validate its efficacy against RSV infections.

Keywords: Human syncytial respiratory virus; Polyvalent multi-epitope vaccine; Immunoinformatics; Molecular docking; Molecular dynamics simulation; Immune simulation

1. Introduction

The Human Respiratory Syncytial Virus (hRSV), a member of the family of *Paramyxoviridae,* is known to be the primary cause of lower respiratory tract infections (LRTI), including

pneumonia and bronchiolitis, in infants, children, as well as elderly and immunocompromised individuals [1-2]. RSV is an enveloped virus that contains a single-stranded, negative-sense RNA with a genome size of about 15.2 kb. As of yet, two major RSV antigenic subtypes have been identified, RSV-A and RSV-B, exhibiting differential sequence divergence throughout their genome; RSV-A has been seen to be more prevalent than RSV-B [2-3]. Antibody cross-reactivity patterns revealed these two antigenic subgroups (A and B) for RSV, which were then divided into genotypes based on genetic divergence within the highly variable G gene [4-6]. Contributory to the fact that the RSV attachment (G) protein has a central conserved domain (CCD) with a CX3C motif, which has been known to be linked to the generation of protective antibodies, vaccine candidates including the G protein are of considerable interest [7]. A novel genotype of RSV-A, known as RSV-A ON1 was found in Ontario, Canada, in 2010. RSV-A ON1 has a 72-nucleotide duplication at the G Protein's C terminus [8], which has been linked to an increased risk of pneumonia and lower respiratory tract infections [9]. However, the two subgroups can coexist and thrive, owing to RSV reinfections being common throughout the life of an infected individual, indicating that cross-immunity against distinct strains is only partial [10]. RSV-A infection is commonly followed by RSV-B infection, although the scenario may vary upon several factors [11]. A claim owing to the antigenic diversity of the G protein states that, both within and between antigenic subgroups, this prominent diversity aids in evading pre-existing host immune responses [12, 13].

RSV severely affects immunocompromised infants and the geriatric population with weaned immune systems. The implicated virus infection is considered globally to be the second largest cause of death, in children under one year of age. RSV-associated acute LRTI is responsible for around 33 million serious respiratory infections a year, according to the World Health Organisation (WHO); resulting in more than 3 million hospitalizations and about 60,000 deaths of children under 5 years of age, and 6.7% of all deaths in infants younger than one-year-old. About a half of these hospitalizations and deaths have since been confirmed to be in infants younger than 6 months of age [14]. Additionally, RSV was identified as the third leading cause of fatal childhood pneumonia after *Streptococcus pneumonia* and *Haemophilus influenza* in 2005, responsible for approximately 66,000 to 199,000 deaths from pneumonia in children younger than 5 years [1]. The consequential impact of RSV on older people may be similar to that of influenza, according to epidemiological research, both in the community and in long-term care institutions. In nursing facilities, attack rates are around 5–10 percent per year, with pneumonia (10–20 percent) and mortality (2–5 percent) being quite common. Moreover, RSV infections cause around 10,000 deaths yearly among those aged 64 and over, according to estimates based on US healthcare databases and viral surveillance results [15]. RSV infects the cells lining the human respiration pathway, including the ciliated epithelial cells, and causes upper and lower respiratory tract complications. Influenza-like diseases and LRTI display clinical symptoms of serious RSV infection. However, the most frequent and serious occurrence of infection in younger children is bronchiolitis. Also, over the lifespan of adults, reinfection by the same and separate strains of RSV is considered to be normal, and therefore, RSV is often termed as a chronic virus [2].

Consequently, over the past two decades, RSV has become a major focus for vaccination studies to decrease the morbidity of lower respiratory tract infections. Several vaccinations and

antiviral drugs have been formulated and implemented over the years since its identification, and while multiple vaccines, prophylactic and monoclonal antibody candidates are available in clinical trials, no approved RSV vaccine is currently available to counter RSV [16]. The first RSV vaccine, composed of the formalin-inactivated virus (FI-RSV) from the Bernett strain, was studied in a clinical trial back in 1966. Unfortunately, however, the FI-RSV vaccine had a disastrous effect as it struggled to induce an effective neutralizing antibody response, thus preventing infection [2]. Large quantities of eosinophils were discovered in the lungs of children and infants with severe illness, but not in individuals who had a normal RSV infection. Following this unanticipated outcome, it was crucial to design a safe RSV vaccine, which included increased testing for vaccine-induced illnesses [17-21]. The inability of the vaccine to elicit effective neutralizing antibodies or memory CD8+ T cells, as well as the production of a significant inflammatory CD4 T cell response, contributed to this vaccine-induced illness [22-25].

Numerous modified RSV vaccine candidates have been designed after the failure of the FI-RSV vaccine trial and many of them are now in clinical trials. However, none of those vaccine candidates being licensed have so far made it to the international economy, for mass production and administration. Although live-attenuated vaccines can stimulate both a humoral and cellular immune response, clinical trials have revealed some potential drawbacks. Chimpanzees are used to compare the amount of attenuation of vaccinations that are candidates for use in humans. Karron et al. found that RSV vaccines that were temperature sensitive and had a high degree of attenuation in chimps could cause infection in the lower respiratory tract in children [26]. Furthermore, recombinant vector-based vaccinations allow for the presentation of one or more antigens encoded on a viral vector such as PIV3 or adenovirus [27]. Intranasal delivery of a new BLP (bacterial-like particle) conjugated to the RSV fusion protein stimulates both mucosal IgA responses and increased IFN-production in a different sort

of vaccination approach [28]. Although both represent effective approaches, further assays to evaluate the long-lasting immune responses are paramount [29].

In addition, it has been observed that, with the use of RSV vaccine candidates, palliative treatment with RSV anti-infective drugs is also required [30]. Merely two approved RSV antivirals are currently available, which include, palivizumab, a humanized preventive monoclonal antibody, and aerosolized ribavirin for therapy. The symptoms of RSV infections can be alleviated by these two antivirals, although they cannot serve prophylactic measures [31]. While studies are underway to identify an effective antiviral therapy or countermeasure to prevent RSV spread and infection, these studies have not been able to deliver any satisfactory findings that can be used to tackle RSV infections [32].

The production of a viable vaccine candidate against a specific pathogen by traditional means can often take many years [33]. However, the age of vaccine production, especially the novel epitope-based "subunit vaccines," has been enriched by today's modern technology and the availability of genomic information for almost all pathogens. These subunit vaccines consist only of the antigenic protein segments of the target pathogen and hence, toxic and immunogenic or allergenic parts of the antigen can be dissipated during the construction of the specific vaccine [34]. Again, the development of vaccines using these computer-based approaches takes far less time, and thus greatly reduces the expense of construction and development [35, 36].

The immunoinformatics approach in this study was used to establish successful polyvalent vaccines against the virulent strains of both forms of RSV, i.e. RSV-A and RSV-B respectively. Immunoinformatics is a vaccine modeling process that allows predictions using several computational methods. The novel antigens of a pathogen or virus are identified in immunoinformatics by dissecting its genomic data and then, through the utilization of various *in silico* biology and bioinformatics tools for vaccine design and development, by analyzing

the target pathogen genome [35, 37]. In our research, a polyvalent epitope-based vaccine blueprint was produced that could produce a significant immune response to both RSV-A and RSV-B forms, targeting the phosphoprotein (P protein), nucleoprotein (N protein), fusion glycoprotein (F protein), and major surface glycoprotein (mG protein) of these viruses. Since RSV-A is more prevalent than RSV-B, as a model, the vaccine was developed using RSV-A [2]. For the T-cell and B-cell epitope prediction, the RSV-A P protein, N protein, F protein, and mG protein were used and then the epitopes with 100 % conservancy in both species along with some other selection criteria were selected for vaccine construction. The criteria for selecting the epitopes include i.e., antigenicity (the parameter that measures whether the epitopes stimulate a high antigenic response), non-allergenicity (to ensure that the epitopes do not cause any unintended allergic reaction inside the body), non-toxicity, conservancy across the selected organisms, as well as non-homologation of the human proteome. It is, therefore, expected that the vaccine will be effective against both the subtypes - RSV-A and RSV-B. The most common vaccine target for RSV is known to be the F protein [574 amino acids (aa) in length], which is a highly conserved protein in both RSV forms. The F protein mediates the fusion and attachment of the virus to its target cells along with the mG protein, thus facilitating viral entry [2, 38]. The F1 (aa 137–574) and F2 (aa 1–109) subunits form a homotrimer in the mature F protein, and the F1 subunit is required for membrane fusion. The F protein has two different conformations i.e., the pre-fusion and post-fusion conformations [39, 40]. The protein rearranges to a more stable post-fusion form during infection to allow viral entrance into the host cell. Antibodies having neutralizing activity identify at least two antigenic sites on both the pre-fusion and post-fusion forms of F (sites II and IV) [41-43]. In this study, the precursor F0 protein was targeted to retrieve all of the potential antigenic epitopes. The possible conformational change of the F protein, as well as the cleavage sites of the protein sequence, were taken into account while generating the potential epitopes [39, 40].

The viral genome of RSV is surrounded by N protein, and the P protein is a vital component of the viral RNA-dependent RNA polymerase complex which is necessary for the proper replication and transcription of RSV [44]. Therefore, in our study, these four proteins were used as possible targets to design a vaccine to suppress these viral proteins, preventing viral entry, and thus interfering with the life cycle of the virus.

2. Methods and Materials

The high throughput immunoinformatics and MD approaches of vaccine designing are illustrated in a step-by-step processes in **Fig 1.**

Fig 1. The step-by-step procedures of immunoinformatics and molecular dynamics approaches used in the vaccine designing study.

2.1. Protein sequences identification and retrieval

Through existing literature reviews in the National Center for Biotechnology Information (NCBI) (https://www.ncbi.nlm.nih.gov/) database, the RSV-A and RSV-B viruses were identified and selected along with their target proteins (i.e., P protein, N protein, F protein, and mG protein). The sequences of target proteins of the selected strains (i.e., RSV strain A2 and RSV strain B1) were then extracted from the UniProt (https://www.uniprot.org/) database in FASTA format. The NCBI Protein database is a collection of SwissProt, PIR, PRF, and PDB sequences. It also includes GenBank, RefSeq, and TPA translations from elucidated coding regions.

2.2. Prediction of antigenicity and analysis of physicochemical properties of the selected proteins

Using the online antigenicity prediction tool, VaxiJen v2.0 (http://www.ddg-pharmfac.net/vaxijen/VaxiJen/VaxiJen.html), the antigenicity of the target protein sequences was predicted with the prediction precision parameter threshold kept at 0.4. This tool uses the method of transformation of auto cross-covariance (ACC) to predict the antigenicity of query proteins or peptides and provides results with an accuracy of 70% to 89%. For this reason, this server is the widely used and accepted server to determine the antigenicity of query proteins [45]. ProtParam tool of the ExPASy server (https://web.expasy.org/protparam/) has subsequently determined numerous physicochemical properties, i.e. the number of amino acids, molecular weight, number of total atoms, theoretical pI, instability index, extinction coefficient, half-life, grand average of hydropathicity (GRAVY), etc. of the target proteins [46].

2.3. Prediction of T-cell and B-cell epitopes

The two major types of T-cells, cytotoxic T-cells, and Helper T-cells are both considered essential for the successful design of the vaccine [47]. For specific antigen recognition of the major histocompatibility complex class I (MHC-I) or CD8+ cytotoxic T-lymphocytic (CTL) epitopes on the surface of the antigen-presenting cells (APCs), the cytotoxic T-cells are important. Additionally, the helper T-cells are considered to be a crucial component of adaptive immunity that interacts on the surface of APCs with major histocompatibility complex class II (MHC-II) or CD4+ helper T-lymphocytic (HTL) epitopes. They function in activating the B-cell, macrophages, and even cytotoxic T-cells [48, 49]. On the other hand, B-cells produce antigen-specific immunoglobulins after their activation [50]. They can identify solvent-

exposed antigens via membrane-bound immunoglobulins called B cell receptors (BCRs) [51]. B-cell epitopes are important for defense against viral infections because they are the essential immune system components that activate an adaptive immune response in response to a specific viral infection. Therefore, the B-cell epitopes are used as one of the crucial building blocks of the subunit vaccine. There are two types of B-cell epitopes: linear B-cell epitopes (LBL) and conformational B-cell epitopes, also known as continuous and discontinuous B-cell epitopes, respectively [52].

The T-cell and B-cell epitope prediction was performed using the Immune Epitope Database or IEDB (https://www.iedb.org/), which contains extensive experimental data on antibodies and epitopes [53]. For the prediction of MHC Class-I or CTL epitopes for several human leukocyte antigen (HLA) alleles, i.e., HLA A*01:01, HLA A*03:01, HLA A*11-01, HLA A*02:01, HLA A*02:06, and HLA A*29:02, the recommended IEDB NetMHCpan 4.0 prediction method was used. The default prediction method selection of the server is 'IEDB recommended' which utilizes the best available technique for a specific MHC molecule based on the availability of predictors and observes the predicted performance for a specific allele. It is updated regularly based on predictor availability. NetMHCpan EL 4.1 is currently used across all alleles for peptide: MHC Class-I binding prediction. Again, for the prediction of MHC class-II or HTL epitopes for DRB1*03:01, DRB1*04:01, DRB1*15:01, DRB3*01:01, DRB5*01:01, and DRB4*01:01 alleles, the recommended IEDB 2.22 prediction method was used. If any corresponding predictor is available for the MHC molecule, the IEDB recommended method employs the Consensus method, combining NN-align, SMM-align, CombLib, and Sturniolo; otherwise, NetMHCIIpan is used. If any three of the four approaches are available, the Consensus approach evaluates them all, with Sturniolo as the final option. Henceforth, based on their ranking, the top-scored HTL and CTL epitopes that were found to be common for all of the selected corresponding HLA alleles were considered for further

analyses. All the parameters were retained by opting for default during the T-cell epitope prediction. Subsequently, B-cell epitopes of the proteins were predicted using the BepiPred linear epitope prediction method 2.0, maintaining all the default parameters. Using a Random Forest algorithm trained on epitope and non-epitope amino acids obtained from crystal structures, the BepiPred-2.0 server predicted linear B-cell epitopes from a protein sequence. Following this, a sequential prediction smoothing was conducted. Residues with scores greater than the threshold (default value of 0.5) were thought to constitute epitopes [54]. Finally, the top-scored LBL epitopes containing more than ten amino acids were primarily regarded as potential candidates for further analysis.

Conformational or discontinuous B-cell epitopes are critical components to induce antibody-mediated humoral immunity within the body. While designing a vaccine, efficient conformational B-cell epitopes should be included alongside the LBLs to elicit a better immunogenic response against the pathogen. The conformational B-cell epitopes of the modeled 3D structure of the vaccine were predicted using IEDB ElliPro, an online server (http://tools.iedb.org/ellipro/) using the default parameters of a minimum score of 0.5 and a maximum distance of 6 angstroms [55]. ElliPro uses three algorithms to predict the protein shape as an ellipsoid, measure the residue PI, and estimate adjacent cluster residues based on their protrusion index (PI) values [56]. ElliPro calculates a score for each output epitope based on an average PI value over the residues of each epitope. Protein residues are contained in 90% of ellipsoids with a PI value of 0.9, while 10% of residues are outside ellipsoids. The center of residue mass residing outside the largest ellipsoid possible was used to calculate the PI value for each epitope residue [57].

2.4. Assessment of antigenicity, allergenicity, toxicity, and topology prediction of the epitopes

In this step, several methods for predicting their conservancy, antigenicity, allergenicity, and toxicity were used to evaluate the initially predicted T-cell and B-cell epitopes. To assess the conservancy of the chosen epitopes [58], the conservancy prediction method of the IEDB server (https://www.iedb.org/conservancy/) was used. Additionally, the components of the vaccine should be highly antigenic, non-allergenic at the same time, and also devoid of toxic reactions. In this step, the antigenicity determination tool VaxiJen v2.0 (http://www.ddg-pharmfac.net/vaxijen/VaxiJen/VaxiJen.html) was used again for the determination of antigenicity [45]. Two different tools were then used, i.e. AllerTOP v2.0 (https://www.ddg-pharmfac.net/AllerTOP/) and AllergenFP v1.0 (http://ddg-pharmfac.net/AllergenFP/) to obtain the highest precision for prediction of allergenicity. Both of the tools are based on auto cross-covariance (ACC) transformation of protein sequences into uniform equal-length vectors. However, the AllerTOP v2.0 server has a better 88.7 % prediction accuracy than the AllergenFP v1.0 server (87.9 %) [59, 60]. In addition, the ToxinPred (http://crdd.osdd.net/raghava/toxinpred/) server was used to predict toxicity for all epitopes by using the Support Vector Machine (SVM) prediction method to keep all the default parameters. The SVM is a widely accepted machine learning technique for toxicity prediction since it can differentiate the toxic and non-toxic epitopes quite efficiently [61]. Finally, using the TMHMM v2.0 server (http://www.cbs.dtu.dk/services/TMHMM/), the transmembrane topology prediction of all the epitopes was performed to predict whether the epitopes were exposed inside or outside, keeping the parameters at their default values. TMHMM uses an algorithm called N-best (or 1-best in this case) to predict the most probable location and orientation of transmembrane helices in the sequence [62].

2.5. Cytokine inducing capacity prediction of the epitopes

Several cytokine types, including IFN-γ, IL-4 (interleukin-4), and IL-10 (interleukin-10) are produced by helper T cells to activate various immune cells, i.e. cytotoxic T cells, macrophages, etc. [63]. As a result, it is crucial to know whether HTL epitopes are capable of producing key cytokines to induce an immune response against the virus before designing a vaccine. The induction capacity of the predicted HTL epitopes for interferon-γ (IFN-γ) was determined using the IFNepitope (http://crdd.osdd.net/raghava/ifnepitope/) server. Based on analyzing a dataset that includes IFN-γ inducing and non-inducing peptides, the server determines the probable IFN-γ inducing epitopes. To determine the IFN-γ inducing capacity, the Design module and the Hybrid (Motif + SVM) prediction approach were used. The Hybrid prediction approach is considered to be a highly precise approach to the prediction of the epitope-inducing capacity of IFN-γ [64]. In addition, IL-4 and IL-10 inducing HTL epitope properties were determined using the servers IL4pred (https://webs.iiitd.edu.in/raghava/il4pred/index.php) and IL10pred (http://crdd.osdd.net/raghava/IL-10pred/) [65, 66]. The SVM method was used on both servers, where the default threshold values were kept at 0.2 and -0.3, respectively.

2.6. Conservancy and human proteome homology prediction

The conservancy analysis of the specified epitopes was conducted using the IEDB server's epitope conservancy analysis module (https://www.iedb.org/conservancy/) [58]. The epitopes that were found to be fully conserved among the selected strains were taken for the construction of the vaccine since this will ensure and facilitate the broad-spectrum activity of the polyvalent vaccine over the two selected RSV species or types. The homology of the human proteome epitopes was determined by the BLAST (BlastP) protein module of the BLAST tool (https://blast.ncbi.nlm.nih.gov/Blast.cgi), where Homo sapiens (taxid:9606) was used for comparison, keeping all other default parameters. An e-value cut-off of 0.05 was set and

358 epitopes were selected as non-homologous pathogen peptides that showed no hits below the e-
359 value inclusion threshold [67]. The epitopes found to be highly antigenic, non-allergenic, non-
360 toxic, fully conserved, and non-homologous to the human proteome were considered among
361 all the initially selected epitopes to be the best-selected epitopes or the most promising epitopes,
362 and only these selected epitopes were used in the construction of the vaccine.

363 2.7. Population coverage and cluster analyses of the epitopes and
364 their MHC alleles

365 A crucial requirement is to consider the distribution of unique HLA alleles among the different
366 populations and ethnicities around the world to design a multi-epitope vaccine since the
367 expression of different HLA alleles can vary from population to population. The IEDB resource
368 for population coverage (http://tools.iedb.org/population/) was used for analyzing the
369 population coverage of the most promising epitopes across several HLA alleles in various
370 regions around the world. Denominated MHC restriction of T cell responses and polymorphic
371 HLA combinations were considered in the analysis. All the parameters were maintained at their
372 default conditions during the study.

373 Furthermore, the human MHC genomic region or HLA is enormously polymorphic, with
374 thousands of alleles; many of which code for a different molecule. MHCcluster is a program
375 that organizes the MHC molecules into functional clusters based on their predicted binding
376 specificity. The approach provides a user-friendly online interface that allows the user to
377 include any MHC in the analysis. A static heat map and graphical tree-based visualizations of
378 the functional relationship between the MHC variants are included in the output as well as a
379 dynamic TreeViewer interface that displays both the functional relationship and the individual
380 binding specificities of the MHC molecules [68]. To evaluate the relationship between the
381 selected MHC alleles, cluster analysis of the MHC alleles was done using the online tool

MHCcluster 2.0 https://services.healthtech.dtu.dk/service.php?MHCcluster-2.0). During the study, 50,000 peptides to be used were retained, 100 bootstrap measurements were retained, and both HLA super-type (MHC Class-I) and HLA-DR (MHC class-II) members were chosen.

2.8. Designing of the multi-epitope subunit vaccine

The most promising antigenic epitopes have been linked with each other to create a fusion peptide using an adjuvant and linkers. Human beta-defensin-3 (hBD-3) used an adjuvant sequence that was linked to the epitopes by EAAAK linkers. Adjuvants are considered to play important roles in improving the antigenicity, immunogenicity, stability, and durability of the developed vaccine. The hBD-3 plays a vital role in host immune responses against the pathogens (i.e., innate mucosal defense within the respiratory tract) and is highly significant against respiratory infections [69-71].

The epitopes were also appended to the pan HLA-DR epitope (PADRE) sequence. By enhancing the ability of CTL vaccine epitopes, the PADRE sequence activates the immune responses [34]. In the conjugation of the CTL, HTL, and LBL epitopes, the AAY, GPGPG, and KK linkers were used, respectively. The EAAAK linkers have a viable partition of bifunctional fusion protein domains [72], while the GPGPG linkers are ideal for preventing junctional epitope production and optimizing the processing and presentation of the immune system [73]. The AAY linker is also commonly used in the design trials of the *in silico* vaccine since this linker offers successful and efficient epitope conjugation [74]. In addition, bi-lysine (KK) linkers are active in the autonomous immunological function of vaccine epitopes [75].

2.9. Physicochemical property analyses of the vaccine with antigenicity and allergenicity test

To build a timely and successful immune response to the pathogenic attack, the constructed vaccine should be strongly antigenic. The antigenicity of the vaccine model was estimated using VaxiJen v2.0 (http://www.ddg-pharmfac.net/vaxijen/VaxiJen/VaxiJen.htm), keeping the threshold value fixed at 0.4 [45]. The findings of the Vaxijen v2.0 server were further cross-checked by the ANTIGENpro module of the SCRATCH protein predictor (http://scratch.proteomics.ics.uci.edu/), holding all the default parameters [76], to achieve better prediction precision. Three separate online methods have estimated the allergenicity of the vaccine structures, i.e. AlgPred (http://crdd.osdd.net/raghava/algpred/), AllerTop v2.0 (https://www.ddgpharmfac.net/AllerTOP/) and AllergenFP v1.0 (http://dg-pharmfac.net/AllergenFP/), to ensure optimum prediction precision. The AlgPred (http://crdd.osdd.net/raghava/algpred/) server aims to combine multiple allergenicity determination methods to reliably determine possible allergenic proteins [77, 78]. To predict the vaccine's allergenicity, the MEME/MAST motif prediction approach was used. The physicochemical properties of the built vaccine were then estimated by the same online instrument, ProtParam (https://web.expasy.org/protparam/)[15], which was previously utilized. The solubility of vaccine constructs was also estimated alongside the physicochemical property study by the SOLpro module of the SCRATCH protein predictor (http://scratch.proteomics.ics.uci.edu/) and later further explained by the Protein-Sol server (https://protein-sol.manchester.ac.uk/). The solubility of a query protein is predicted by all these servers with remarkable precision. SolPro produces its predictions based on the SVM method, while Protein-Sol uses a rapid method of deciding the results based on sequence [76, 79]. All the parameters of the servers were maintained at their default values during the solubility review.

2.10. Secondary and tertiary structure prediction of the vaccine construct

The vaccine construct was subjected to secondary structure prediction following physicochemical analysis. For this, several online resources were used to preserve all the default parameters, i.e. PSIPRED (http://bioinf.cs.ucl.uk/psipred/) (using the PSIPRED 4.0 prediction method), GOR IV (https://npsa-prabi.ibcp.fr/cgibin/npsa automat.pl?page=/NPSA/npsa gor4.html), SOPMA (https://npsa-prabi.ibcp.fr/cgibin/npsa automat.pl?page=/NPSA/npsa sopma.html) and SIMPA96 (https://npsaprabi.ibcp.fr/cgibin/npsa automat.pl?page=/NPSA/npsa npsa.html) and SIMPA96 (https://npsa.npsa.npsa.npsa.npsa. To predict the percentages or quantities of amino acids in α helix, β-sheet, and coil structure formations, these servers are considered to be reliable, quick, and effective [80-84]. Moreover, determination of the tertiary or 3D structure of the vaccine construct was carried out using the RaptorX online server (http://raptorx.uchicago.edu/). Using an easy and powerful template-based method [85], the server predicts the tertiary or 3D structure of a query protein. Furthermore, RaptorX uses a deep learning method to enable distance-based protein folding. This server has also been rated first in contact prediction in both CASP12 and CASP13, making it an ideal server for 3D structure determination [86].

2.11. Refinement and validation of tertiary structure of the vaccine

The tertiary structure prediction of the proteins using computational methods also requires extensive refinement, to turn predicted models with lower resolution into models that closely match the native protein structure. Therefore, a GalaxyWEB server (http://galaxy.seoklab.org/) using the GalaxyRefine module further refined the created tertiary structure of the proposed vaccine model. The server uses dynamic simulation and the refinement approach is tested by CASP10 to refine the tertiary protein structures [87, 88]. Furthermore, validation of the refined protein was carried out by analyzing the Ramachandran plot created by the PROCHECK (https://servicesn.mbi.ucla.edu/PROCHECK/) tool [89, 90]. Along with PROCHECK for protein validation, another online platform, ProSA-web

(https://prosa.services.came.sbg.ac.at/prosa.php) was also used. A z-score that expresses the consistency of a query protein structure is created by the PROCHECK server. In the latest PDB database, a z-score residing within the z-score spectrum of all experimentally defined protein chains represents a higher consistency of the query protein [91].

2.12. Vaccine protein disulfide engineering analysis

Disulfide bonds are more likely to form in a few regions within a protein structure, providing stability through reduced conformational entropy and increased free energy concerning the denatured state. However, disulfide engineering is the process of introducing disulfide bonds to a target protein to increase its stability. In this experiment, the Disulfide by Design (DbD)2 v12.2 (http://cptweb.cpt.wayne.edu/DbD2/) online tool was used to predict the locations and further design the disulfide bonds within the vaccine proteins [92]. The tool was developed using computational approaches to predict the protein structure [93, 94], and the algorithm of this server accurately estimates the χ3 torsion angle based on 5the Cβ–Cβ distance using a geometric model derived from native disulfide bonds. The Caf-Cβ-Sγ angle is allowed some tolerance in the DbD2 server based on the wide range found in native disulfides. To facilitate the ranking process, DbD2 estimates an energy value for each potential disulfide and mutant PDB files may be generated for selected disulfides [95].

The χ3 angle was held at -87 ° or +97 ° ±10 during the experiment to cast off various putative disulfides that were generated using the default angles of +97 ° ±30 ° and -87 ° ±30 °. Additionally, the angle of Caf-Cβ-Sγ was set to its default value of 114.6° ±10. Finally, to allow disulfide bridge formation, residue pairs with energy less than 2.2 Kcal/mol were selected and mutated to cysteine residue [96]. The energy value of 2.2 Kcal/mol was chosen as the disulfide bond selection threshold since 90% of native disulfide bonds are usually considered to have an energy value of less than 2.2 Kcal/mol [92].

2.13. Post-translational modification analysis

For posttranslational modification analysis of the vaccine construct comprising of the B-cell and T-cell epitopes, the NetNGlyc-1.0 (http://www.cbs.dtu.dk/services/NetNGlyc-1.0), NetOGlyc4.0 (http://www.cbs.dtu.dk/services/NetOGlyc-4.0), and NetPhos-3.1 (http://www.cbs.dtu.dk/services/NetPhos-3.1) servers were utilized. The NetNglyc server uses artificial neural networks to predict N-glycosylation sites in human proteins by examining the sequence context of Asn-Xaa-Ser/Thr sequons [97]. Any potential that exceeds the default threshold of 0.5 indicates a predicted glycosylated site. The average output of nine neural networks is used to get the 'potential' score. The NetOglyc server (http://www.cbs.dtu.dk/services/NetOGlyc-4.0) predicts mucin type GalNAc O-glycosylation sites in mammalian proteins using neural networks [98].

This server provides a list of probable glycosylation sites for each input sequence, together with their positions in the sequence and prediction confidence scores. Only locations with a score greater than 0.5 are expected to be glycosylated and the string "POSITIVE" is added to the remark box. Using ensembles of neural networks, the NetPhos 3.1 server (http://www.cbs.dtu.dk/services/NetPhos-3.1) predicts serine, threonine, or tyrosine phosphorylation sites in eukaryotic proteins. Predictions are made for both generic and kinase-specific kinases. A prediction score greater than 0.5 indicates a positive prediction.

2.14. Analysis of protein-protein docking

The vaccine protein was docked against several toll-like receptors (TLRs) in protein-protein docking analysis. A strong binding affinity should be present between the vaccine and the TLRs. This is crucial because, after identifying the vaccine that resembles the initial viral infections, TLR proteins generate possible immune responses, and thus help to produce immunity against the pathogen [99]. In this study, different TLRs have been docked with the

vaccine protein, i.e. TLR-1 (PDB ID: 6NIH), TLR-2 (PDB ID: 3A7C), TLR-3 (PDB ID: 2A0Z), TLR-4 (PDB ID: 4G8A), and TLR9 (PDB ID: 3WPF). ClusPro v2.0 (https://cluspro.bu.edu/login.php) was used to conduct the docking, where the lower energy score corresponds to the stronger binding affinity. Based on the following equation, the ClusPro server calculates the energy score:

$$\boldsymbol{E = 0.40Erep + (-0.40Eatt) + 600Eelec + 1.00EDARS\,[54-55]}.$$

The repulsions and attraction energies owing to van der Waals interactions are denoted by E_{rep} and E_{attr}, respectively, whereas E_{elec} signifies the electrostatic energy component. The Decoys' pairwise structure-based potential is represented by E_{DARS} as the Reference State (DARS) method. Furthermore, another round of docking was carried out using the ZDOCK server which is a rigid-body protein-protein docking tool that employs a combination of shape complementarity, electrostatics, and statistical potential terms for scoring and uses the Fast Fourier Transform algorithm to enable an efficient global docking search on a 3D grid. In the most current benchmark version (Accelerating protein docking in ZDOCK utilizing an advanced 3D convolution library), ZDOCK achieves high predictive accuracy on protein-protein docking benchmarks, with >70 % success in the top 1000 predictions for rigid-body instances [100].

2.15. Molecular dynamics simulation studies and MM-PBSA calculations

The docked complexes from the ZDOCK server were used in MD simulations. The complexes being protein-protein in nature with multiple chains, the MD simulations were computationally expensive and performed on the HPC cluster at Bioinformatics Resources and Applications Facility (BRAF), C-DAC, Pune with Gromacs 2020.4 [101] MD simulation package. The CHARMM-36 force field parameters [102, 103] were employed to prepare the topology of

protein chains. The system of each TLR along with the bound vaccine was solvated with the single point charge water model [104] in the dodecahedron unit cells and neutralized with the addition of Na^+ or Cl^- counter-ions. The solvated systems were initially energy minimized to relieve the steric clashes if any with the steepest descent criteria until the threshold (Fmax< 10 kJ/mol) was reached. These energy minimized systems were then equilibrated at constant volume and temperature conditions 300 K using modified Berendsen thermostat [105] and then at constant volume and pressure Berendsen barostat [106] for 100 ps each. The equilibrated systems were later subjected to 100 ns production phase MD simulations, where the modified Berendsen thermostat and Parrinello-Rahman barostat [107] were used with covalent bonds restrained using the LINCS algorithm [108]. The long-range electrostatic interaction energies were measured with the cut-off of 12 Å, with the Particle Mesh Ewald method (PME) [109]. The resulting trajectories were analyzed for root mean square deviations (RMSD) in protein backbone atoms, root mean square fluctuations (RMSF) in the side chain atoms of individual chains in each protein complex, the radius of gyration (Rg), and several hydrogen bonds formed between vaccine protein chain and the respective TLR protein chain.

2.16. Immune simulation studies

To forecast the immunogenicity and immune response profile of the proposed vaccine, an immune simulation analysis was performed. For the immune simulation study, the C-ImmSim server (http://150.146.2.1/CIMMSIM/index.php) was used to predict real-life immune interactions using machine learning techniques and PSSM (Position-Specific Scoring Matrix) [110]. During the experiment, all the variables except for the time steps were kept at their default parameters. However, the time steps at 1, 84, and 170 were retained (time step 1 is injection at time = 0), and the number of simulation steps was set to 1050. Thus, three injections at four-week intervals were administered to induce recurrent antigen exposure [111].

2.17. Codon adaptation and *in silico* cloning within *E.coli* System

Codon adaptation and *in silico* cloning are two significant steps that are conducted to express multi-epitope vaccine construction within an *Escherichia coli* (*E.coli)* K12 strain. In different organisms, an amino acid can be encoded by more than one codon, which is known as codon bias wherefore, the codon adaptation study is carried out to predict an appropriate codon that effectively encodes a specific amino acid in a specific organism. Java Codon Adaptation Tool or JCat server (http://www.jcat.de/) was used for codon optimization [112], and the optimized codon sequence was further analyzed for expression parameters, codon adaptation index (CAI), and GC-content %. The optimum CAI value is 1.0, while a score of > 0.8 is considered acceptable, and the optimum GC content ranges from 30 to 70% [113]. For *in silico* cloning simulation, the pETite vector plasmid was selected which contains a small ubiquitin-like modifier (SUMO) tag as well as a 6x polyhistidine (6X-His) tag, which will facilitate the solubilization and affinity purification of the recombinant vaccine construct [114]. Also, 6X-His can facilitate the swift detection of the recombinant vaccine construct in immunochromatographic assays [115]. The vaccine protein sequence was reverse-translated to the optimized DNA sequence by the server to which EaeI and StyI restriction sites were incorporated at the N-terminal and C-terminal sites, respectively. The newly adapted DNA sequence was then inserted between the EaeI and StyI restriction sites of the pETite vector using the SnapGene restriction cloning software (https://www.snapgene.com/free-trial/) to confirm the expression of the vaccine [116, 117].

2.18. Prediction of the vaccine mRNA secondary structure

Two servers, i.e. Mfold (http://unafold.rna.albany.edu/?q=mfold) and RNAfold (http://rna.tbi.univie.ac.at/cgibin/RNAWebSuite/RNAfold.cgi), were used for the mRNA secondary structure prediction. Both of these servers thermodynamically predict the mRNA

574 secondary structures and provide each of the generated structures with minimum free energy
575 ('G Kcal/mol'). The more stable the folded mRNA is, the lower the minimum free energy and
576 vice versa [55][118-120]. To analyze the mRNA folding and secondary vaccine structure, the
577 optimized DNA sequence was first taken from the JCat server and converted via the DNA<-
578 >RNA->Protein tool (http://biomodel.uah.es/en/lab/cybertory/analysis/trans.htm) to a possible
579 RNA sequence. The RNA sequence was then gathered from the tool and utilized for prediction
580 into the Mfold and RNAfold servers using the default settings for all the parameters.

581

582 3. Results

583 3.1. Protein sequences identification and retrieval

584 From the NCBI database, the RSV viral strains and the query proteins were identified.
585 Following that, the four RSV-A and RSV-B Query Proteins including P protein, N protein, F
586 protein, and mG, were retrieved from the UniProt online database. The UniProt Accession
587 Number and the length of the query proteins are listed in **Table 1**.

588

589 **Table 01.**

Name of the Virus	Name of the Protein	UniProt Accession Number of the Protein	Length (aa) of the Protein Sequence
RSV-A	P protein	P03421	241
	N protein	P03418	391
	F protein	P03420	574
	mG protein	P03423	298
RSV-B	P protein	O42062	241
	N protein	O42053	391

	F protein	O36634	574
	mG protein	O36633	299

List of the proteins with their accession numbers used in the vaccine designing study.

3.2. Prediction of antigenicity and analysis of physicochemical properties of the selected proteins

The selected proteins were analyzed for antigenicity and physicochemical properties through the VaxiJen v2.0 server and ProtParam tool of the ExPASy server, respectively. To be a vaccine candidate, antigenicity is a prerequisite for a protein or amino acid sequence. All of the selected proteins were found to be antigenic in VaxiJen v2.0 server at threshold 0.4. In addition, while P protein and N protein of RSV-A and RSV-B were found to have an acidic theoretical pI (pH lower than 7), F protein and mG protein were found to have a basic theoretical pI (pH higher than 7). The protein having an acidic theoretical pI belongs to negatively charged proteins. Again, in the mammalian cell culture system, all the query proteins had a similar half-life of 30 h and a high aliphatic index (over 60.00) as well. All of the proteins had quite low GRAVY values (lower than -0.909)**.** P protein of the RSV-A and RSV-B had the highest GRAVY value of -0.909 and -0.827, respectively. Whereas, the F protein of RSV-A and RSV-B had the lowest GRAVY value of -0.028 and -0.033, respectively. Furthermore, the F protein of the RSV-A and RSV-B had the highest aliphatic index of 99.97 and 102.35, respectively. **S1 Table** lists the results of the analysis of physicochemical properties of all the query proteins.

3.3. Epitope prediction and sorting the most promising epitopes

The RSV-A proteins were selected as models during the prediction of the T-cell and B-cell epitopes by the IEDB server for the construction of the polyvalent vaccine, meaning that the

611 epitopes were selected using only the RSV-A proteins and then only the fully conserved
612 epitopes were taken therefore, the epitopes should confer immunity to the selected strains of
613 both RSV-A and RSV-B. These epitopes were anticipated to induce potential T-cell and B-cell
614 immune responses after the vaccine administration. Based on the ranking, the top CTL and
615 HTL epitopes as well as top B-cell epitopes with lengths over ten amino acids were taken into
616 consideration for further analysis. Following this, a few criteria were selected to filter the best
617 epitopes which included, high antigenicity, non-allergenicity, non-toxicity, conservancy, and
618 human proteome non-homology. Furthermore, the cytokine (i.e., IFN-γ, IL-4, and IL-10)
619 inducing ability of HTL epitopes was also considered to determine whether they can produce
620 at least one of these cytokines. Finally, the epitopes that met these criteria were listed as the
621 most promising epitopes in **Table 02** and were later used for the construction of the vaccine.
622 The analysis of transmembrane topology by the TMHMM v2.0 server of the most promising
623 epitopes revealed that PEFHGEDANNR, SFKEDPTPSDNPFS, EVAPEYRHDSPD,
624 VFPSDEFDASISQVNEK,
625 IPNKKPGKKTTTKPTKKPTLKTTKKDPKPQTTKSKEVPTTKP were exposed outside.

626 **S2 Table** listed the potential epitopes of P protein and **S3 Table** listed the potential epitopes of
627 N protein. The potential epitopes of F protein are listed in **S4 Table** and the potential epitopes
628 of mG protein are listed in **S5 Table.**

629

630 **Table 02**.

Name of the Protein	MHC class-I epitopes	MHC class-II epitopes	B cell epitopes
P protein	VSLNPTSEK	LGMLHTLVVASAGPT	PEFHGEDANNR
	QTNDNITAR	LHTLVVASAGPTSAR	EVTKESPITSNSTIINPTNETDDTAGNKPNYQRK
	-	-	SFKEDPTPSDNPFS

	-	-	RNEESEKMAKDTSDEVSLNPTSEK
N protein	CIAALVITK	EVLTLASLTTEIQIN	EVAPEYRHDSPD
	RSGLTAVIR	-	EYRGTPRNQDLYDA
	SVKNIMLGH	-	-
F protein	KTNVTLSKK	IVIIVILLSLIAVGL	VFPSDEFDASISQVNEK
	KSALLSTNK	VIIVILLSLIAVGLL	-
	IASGVAVSK	EEFYQSTCSAVSKGY	-
	KQLLPIVNK	-	-
	ITIELSNIK	-	-
	LTSKVLDLK	-	-
mG protein	TTTQTQPSK	LSILAMIISTSLIIA	TSQIKNTTPTYLTQNPQLGISPSNPSEITS
	IFIASANHK	TLSILAMIISTSLII	IPNKKPGKKTTTKPTKKPTLKTTKKDPKPQTTKSKEVPTTKP TEEPTINTT
	-	QNPQLGISPSNPSEI	SNTTGNPELTSQ

List of the epitopes eventually selected for the construction of the vaccine (selection criteria: antigenicity, non-allergenicity, non-toxicity, 100 % conservancy and non-homolog to the human proteome).

3.4. Population coverage and cluster analyses of the epitopes and their MHC alleles

The population coverage analysis showed that 85.70% and 87.92% of the world population were covered by the MHC class-I and class-II alleles and their epitopes, respectively, and 84.62% of the world population was covered by the combined MHC class-I and class-II. While India had the highest percentage of population coverage for the CTL epitopes (87.56 %) as well as HTL epitopes (93.51 %), China had the highest percentage of population coverage for CTL and HTL epitopes in combination (91.80 %) (**Fig 2**).

644 **Fig 2.** The result of the population coverage analysis of the most promising epitopes and their
645 selected MHC alleles

646

647 Cluster analysis of the potential alleles of MHC class I and MHC class II that may interfere
648 with the predicted epitopes of the RSV query proteins was also conducted. The study was
649 carried out using the online tool MHCcluster 2.0, which phylogenetically demonstrates the
650 relation of the allele clusters. **S1 Fig** shows the outcome of the experiment where a strong
651 interaction is shown in the red zone and a weaker interaction in the yellow zone.

652 3.5. Designing of the multi-epitope subunit vaccine

653 The most promising T-cell and B-cell epitopes were used to design the multi-epitope vaccine
654 incorporating adjuvant and appropriate linkers. The hBD-3 was used as an adjuvant to design
655 the vaccine and the PADRE sequence was also used as a potent inducer of immunity. The
656 adjuvant was linked with the epitopes by the EAAAK linker. Furthermore, AAY, GPGPG, and
657 KK were used to associate the epitopes with each other at their appropriate positions as given
658 in **Fig 3.**

659

660 **Fig 3.** (A) Schematic representation of the potential vaccine construct with linkers (EAAAK,
661 AAY, GPGPG, and KK), PADRE sequence, adjuvant (hBD-3) and epitopes (CTL, HTL, and LBL)
662 in a sequential and appropriate manner (B) Sequence of the vaccine protein. The letters in bold
663 represent the linker sequences.

664

665 3.6. Prediction of antigenicity, allergenicity and Physicochemical
666 property analysis of the vaccine

The vaccine protein was observed to be both a potent antigen and a non-allergen. The vaccine had a high theoretical (basic) pI of 9.75. It had a reasonably adequate half-life in mammalian cells of 30 h and of more than 10 h in the *E. coli* cell culture system. The GRAVY value of the vaccine was considered to be significantly negative at -0.362. Additionally, both servers, Sol-Pro and Protein-sol, have also shown that the vaccine protein is soluble, attesting to its negative value. The instability index of the protein was found to be less than 40 (27.55), indicating the vaccine to be quite stable. The extinction coefficient and the aliphatic index of the vaccine were also found to be high with values, 45770 M^{-1} cm^{-1} and 80.85, respectively.

3.7. Secondary and tertiary structure prediction of the vaccine

The secondary structure of the vaccine protein revealed that the coil structure had the largest number of amino acids, while the β-strand showed the lowest percentage. The predictions provided by all four servers are depicted in **Fig 4**. The amino acid percentages of α-helix, β-strand, and coil structure of the vaccine protein produced from four different servers are listed in **Table 03**. All of the servers revealed almost similar predictions and the overall analysis also showed that the adjuvant generated potential variations in the secondary structure of the vaccine protein. The vaccine construct's 3D structure was predicted by the RaptorX online server. The constructed vaccine protein had a surprisingly low p-value of 8.71e-05 in 4 domains, which demonstrated that the accuracy of the proposed 3D structure was significantly good. Using 1KJ6A as the template from the Protein Data Bank, the homology modeling of the vaccine construct was completed. Furthermore, the vaccine structure was modeled using Modeller, as shown in **Fig 5**, to further improve the quality.

Table 03.

Secondary structure elements	PRISPRED	GOR IV	SOPMA	SIMPA96
α-helix	33.51%	32.98%	30.56%	29.61%

β-strand	16.22%	15.58%	18.46%	14.50%
Coil structure	50.25%	51.44%	50.98%	55.74%

Results of the secondary structure analysis of the vaccine construct.

Fig 4. The results of the secondary structure prediction of the vaccine. (A) PRISPRED prediction, (B) GOR IV prediction, (C) SOPMA prediction, (D) SIMPA96 prediction.

Fig 5. (A) The tertiary or 3D structure of the vaccine construct modeled, refined and visualized by RaptorX, GalaxyWEB server, and BIOVIA Discovery Studio Visualizer v. 17.2 respectively. (B) The results of the Ramachandran plot analysis generated by PROCHECK server and (C) quality score or z-score graph generated by the ProSA-web server of the refined vaccine construct. In the Ramachandran plots, the orange and deep yellow colored regions are the allowed regions, the light yellow regions are the generously allowed regions and the white regions are the outlier regions and the glycine residues are represented as triangles.

3.8. Refinement and validation of tertiary structure of the vaccine

The 3D structure of the vaccine protein produced by the RaptorX server was refined to predict a structure that closely resembles the native protein structure. The refined protein structure was then validated by evaluating the PROCHECK server-generated Ramachandran plot and the ProSA-web server-generated z-score. The Ramachandran plot study found that in the most preferred region, the vaccine protein had 93.5 % of amino acids, while in the additional approved regions, 5.4 % of amino acids, 0.4 %of amino acids in the generously permitted regions, and 0.7 % of amino acids in the disallowed regions. In comparison, the z-score of the engineered vaccine was -6.58, which is beyond the range of all experimentally confirmed X-ray crystal protein structures from the Protein Data Bank. The protein validation analysis estimated that there was a reasonably good consistency structure in the distilled form (**Fig 5**).

3.9. Prediction of conformational B-lymphocytic epitopes

The conformational B-cell epitopes of the vaccine protein were predicted using the ElliPro server which predicts conformational epitopes from tertiary structures of the protein. A score of 0.50 or higher was selected for the prediction of discontinuous peptides by Ellipro. Three discontinuous B-cell epitopes were predicted to include 333 amino acid residues, with values ranging from 0.506 to 0.675. The size of the conformation epitopes varied from 4 to 394 residues. Three-dimensional representation of conformational B cell epitopes of the designed multi-epitope-based RSV vaccine and the epitope residues are shown in **Fig 6** and listed in **S6 Table.**

Fig 6. Graphical representations of the predicted conformational B-cell epitopes of the modeled vaccine indicated by yellow coloured ball-shaped structures.

3.10. Vaccine protein disulfide engineering analysis

The disulfide bonds of the vaccine structure were predicted using the DbD2 server in protein disulfide engineering. Based on certain classification criteria, the server recognizes pairs of amino acids with the ability to form disulfide bonds. Only those amino acid pairs that had bond energy smaller than 2.2 kcal/mol were chosen in this experiment. Three pairs of amino acids with bond energy below 2.2 kcal/mol were provided by the RSV: 23 Cys and 38 Cys, 414 Ala and 414 Lys, and 513 Tyr- 516 Thr. The selected pairs of amino acids have formed the mutant vaccine in the DbD2 server, which contains potential disulfide bonds within (**S2 Fig**). This indicates the probable stability of the designed multi-epitope vaccine construct.

3.11. Post-translational modification analysis

The posttranslational modification analysis was performed to see whether the vaccine construct would undergo any substantial changes after being administered to mammalian cells. Four N-glycosylation sites and sixty-three O-glycosylation sites were predicted in the vaccine construct sequence. The findings suggest that a significant amount of glycosylation may have occurred inside the predicted vaccine construct, which might improve the vaccine's efficacy and immunogenicity. In addition, the vaccine protein sequence has ninety-six phosphorylated residues (i.e., serine residues (S), threonine (T), and tyrosine (Y) phosphorylation sites) according to the NetPhos v2.0 server output. The server-provided plots containing the N-glycosylation sites and phosphorylation are given in **S3 Fig.**

3.12. Analysis of protein-protein docking

Protein-protein docking analysis was performed to demonstrate the vaccine's ability to interact with various crucial molecular immune components i.e., TLRs. When docked using ClusPro 2.0, it demonstrated very high binding affinities with all its targets (TLRs). It has been further studied using the ZDOCK server where the vaccine protein also displayed very strong interaction with the TLRs. The lowest energy level obtained for docking between the vaccine construct and TLR-1, TLR-2, TLR-3, TLR-4, and TLR-9 were -986.1, -1236.7, -1084.4, -1260.8, and -1226.4, respectively. The lowest energy level between the vaccine and TLRs indicated the highest binding affinity.

3.13. Molecular dynamics simulation studies and MM-PBSA calculations

MD simulation is an effective method for the analysis of biological systems and it provides many mechanistic insights into the possible behavior of the system under a simulated biological

environment [121]. Gromacs 2020.4 was used to carry out the production phase MD and the analysis of resulting trajectories was undertaken to understand the structural properties, and interaction between different TLRs and the predicted vaccine protein at a molecular level. The snapshots of equilibrated structures of each TLR-vaccine complex and the snapshots of the last trajectories are shown in **Fig 7**. The visual inspection of trajectories at different time intervals suggested that the side chains of the vaccine make different interactions with chain A of all TLRs except TLR1, where vaccine side chains were found to be interacting with side chains of both A and B chains.

Fig 7. Snapshots of equilibrated (initial) systems and last trajectories. Vaccine bound complexes of A) TLR1, B) TLR2, C) TLR3, D) TLR4, and E) TLR9 (For each snapshot the surface representation and cartoon representations are shown)

Root mean square deviations (RMSD) analysis gives insights into how the backbone atoms move relative to the initial equilibrated positions. Lower the RMSD, better the stability of the corresponding system. In the present work, we measured the RMSD in backbone atoms of entire protein-protein complexes of TLRs with a vaccine. **Fig 8A** shows the RMSD in the investigated systems. The evaluation of root means square fluctuations (RMSF) provides insights into the possible changes in the secondary structure of protein under investigation. In the present work, the RMSF in the side chain atoms of residues in each system was measured. As the TLR-vaccine systems have multiple chains, the RMSF evaluation is performed on each chain of the complex to understand which residues are involved in the key contacts. The RMSF in the TLR side-chain atoms is shown in **Fig 8B**. The RMSF in other chains in each of the TLRs is given in **S4 Fig.** The analysis of radius of gyration (Rg) provides the overall measurement of compactness of the system [122]. The results of total Rg are shown in **Fig 8C**.

Analysis of non-bonded interactions such as hydrogen bonds is quite challenging in protein-protein complexes. The side chains of the proteins participate in hydrogen bond interactions. The hydrogen bond analysis of all the trajectories was performed with the h-bond module of Gromacs, while the key residues at the interface of the TLR chain and vaccine chain were analyzed through the chimeraX program [123]. The results of the hydrogen bond analysis are shown in **S5 Fig**.

Fig 8: Results of the (A) Root mean square deviations in the investigated systems, (B) Root mean square fluctuations in the side chain atoms of vaccine, and (C) Radius of gyration of the vaccine.

3.14. Immune simulation studies

The immune simulation study of the designed vaccine was conducted using the C-ImmSimm server which forecasts the activation of adaptive immunity as well as the immune interactions of the epitopes with their specific targets [63]. The analysis exhibited that the primary immune reaction to the vaccine could be stimulated substantially after administration of the vaccine, as demonstrated by a steady rise in the levels of different immunoglobulins i.e., (IgG1 + IgG2, and IgG + IgM antibodies) (**Fig 9A**). It was also expected that the concentrations of active B cells (**Fig 9B** and **Fig 9C**), plasma B cells (**Fig 9D**), helper T cells (**Fig 9E** and **Fig 9F**), and cytotoxic T cells (**Fig 9H** and **Fig 9I**) could steadily increase, reflecting the vaccine's capacity to create a very high secondary immune response and healthy immune memory. However, **Fig 9G** demonstrates that the concentration of regulatory T cells would gradually decrease throughout the phases of the injections, which represents the decrease in suppression of vaccine-induced immunity by regulatory T cells [124].

In comparison, the rise in macrophage and dendritic cell concentrations showed that these APCs had a competent presentation of antigen (**Fig 9J** and **Fig 9K**). The simulation result also

807 predicted that the constructed vaccine could generate numerous forms of cytokines, including
808 IFN-γ, IL-23, IL-10, and IFN-β; some of the most critical cytokines for producing an immune
809 response to viral infections (**Fig 9L**). Therefore, the overall immune simulation analysis
810 showed that after administration, the proposed polyvalent multi-epitope vaccine would be able
811 to elicit a robust immunogenic response.

812 3.15. Codon adaptation, *in silico* cloning, and interpretation of the
813 vaccine mRNA secondary structure

814 The protein sequence of the vaccine was adapted by the JCat server for *in-silico* cloning and
815 plasmid construction. The CAI value was found to be 0.98, suggesting that the DNA sequences
816 contained a larger proportion of the codons most likely to be included in the target organism's
817 (K12 strain of *E.coli*) cellular machinery [118, 119]. Furthermore, GC content of the formed
818 sequence was found to be 50.23 %, within the desired range. The graph demonstrating the
819 sequence after codon adaptation is shown in **S6 Fig**. Following codon adaptation, the projected
820 vaccine DNA sequence was inserted between the EaeI and StyI restriction sites into the pETite
821 vector plasmid. The plasmid includes SUMO and 6X H tag sequences that are required to
822 promote the vaccine's purification during downstream processing [125]. The newly built
823 recombinant plasmid has been designated as “Cloned_ pETite" (**Fig 10**). Thereafter, the Mfold
824 and RNAfold servers predicted the secondary structure of the vaccine mRNA. A minimum free
825 energy score of -549.30 kcal/mol was produced by the Mfold server, which was consistent with
826 the prediction of the RNAfold server that also predicted a minimum free energy of -526.30
827 kcal/mol. In **S7 Fig**, the vaccine mRNA secondary structure is depicted.

828

829 **Fig 10**. *In-silico* cloning of the vaccine sequence in the pETite plasmid vector. The codon
830 sequence of the final vaccine is presented in red generated by the JCat server. The pETite
831 expression vector is in black.

832

833 4. Discussion

834 hRSV is conventionally the most prevalent cause of human LRTIs, known to infect individuals
835 from all age groups but more commonly newborns and children. Implicated infections of RSV
836 contribute to affecting and killing numerous people all over the globe, yet no pre-existing
837 authorized vaccine is recognized as an effective measure to prevent RSV infections. Vaccines
838 are extensively used to control and prevent diseases caused by a variety of pathogens across
839 the world. Conventional methods are primarily used for vaccine development and manufacture,
840 despite the associated disadvantages of being expensive and time-consuming [126]. In contrast
841 to traditional vaccine production strategies, today's cutting-edge research and technology as
842 well as the availability of knowledge about the genome and proteome of almost all viruses and
843 organisms, facilitate the design and development of novel peptide-based subunit vaccines.
844 Subunit vaccines have the benefit of being able to eliminate toxic and immunogenic
845 components of an antigen during a vaccine design study, making the vaccine safe to administer
846 in people. Subunit vaccines include a limited amount of viral particles that cause patients to
847 develop protective immunity. A subunit vaccine is a cost-efficient and effective way to prevent
848 health concerns [127-129]. As a result, bioinformatics and immunoinformatics techniques have
849 been developed and widely utilized to design novel subunit vaccines that are safe, effective,
850 efficient, and low-cost alternatives to current preventive measures [130, 131].

851

The narrated experiment utilized immunoinformatics methods to design a blueprint of a polyvalent epitope-based vaccine against the antigenic subgroups, RSV-A and RSV-B, targeting four distinctive proteins which include - P protein, N protein, F protein, and mG protein. Antigenicity and physicochemical properties of the proteins were predicted, where all the proteins identified were shown to be antigenic; a requirement for the use of a target protein in epitope-based vaccine construction. The theoretical pI represents the pH at which there is no net effective charge and mobility in a protein as well as predicts whether a protein is basic or acidic [132]. The instability index of a protein represents the likelihood of that specific compound being stable, and a compound with an instability index greater than 40 is deemed unstable [133]. The aliphatic index measures the relative amount of amino acids occupied by aliphatic amino acids in its side chains [134]. The high aliphatic index also indicates the improved thermal stability of a protein [135]. All of the query proteins had a high extinction coefficient and theoretical half-life of 30 h in mammalian cells. The extinction coefficient indicates the ability of a protein to absorb light at a certain wavelength and a higher extinction coefficient represents the higher absorbance of light by the protein [136, 137]. The GRAVY value represents a compound's hydrophilic or hydrophobic traits. The GRAVY negative value reflects hydrophilic characteristics, while the GRAVY positive value reflects the hydrophobic characteristics of the compound [138, 139]. Since all query proteins were found to be quite antigenic having a high aliphatic index and extinction coefficient, as well as negative GRAVY values, they were expected to be thermostable, high light-absorbing as well as hydrophilic in nature. Overall, the physiological property analyses of the proteins revealed satisfactory results, desired for the epitope predictions. CTL, HTL, and LBL epitopes are some mandatory constituents for a multi-epitope subunit vaccine, known to stimulate or activate the cytotoxic T-cells, helper T-cells, and B-cells to generate an effective host immune response [140]. Cytotoxic T-cells can recognize the foreign antigens while helper T-cells recruit the other

877 immune cells including B-cells, macrophages, and even cytotoxic T-cells to ensure the
878 generation of immune responses [38, 48]. In addition, B-cells mediate the humoral immune
879 response by producing immunoglobulins or antibodies that are antigen-specific [50][141, 142].

880 Once the vaccine protein reaches the host antigen-presenting cells (APC), they are processed,
881 and the T cell epitopes are proteolytically cleaved off the protein, which is then represented by
882 MHC molecules on the surface of APCs, exposing them to T cell receptors [143]. MHC class
883 I molecules represent endogenous antigens often referred to as epitopes, such as intracellular
884 proteins of a pathogen (e.g., bacteria or virus) or any tumor-inducing proteins whereas, MHC
885 class II molecules represent exogenous epitopes. Furthermore, the antigen region that binds to
886 the immunoglobulin or antibody is referred to as the B-cell epitope. These B-cell epitopes can
887 be found in any exposed solvent area of the antigen and can be of various chemical types. The
888 majority of antigens, however, are proteins, which are the targets of epitope prediction
889 algorithms. The goal of B-cell epitope prediction is to ensure a more convenient method to
890 identify B-cell epitopes, to substitute antigen for antibody production by the plasma B-cells, or
891 conduct structure-function studies. Thus, antibodies can recognize any area of the antigen that
892 has been exposed to solvents. B-cell epitopes can be split into two categories: linear and
893 conformational; conformational B-cell epitopes are made up of patches of solvent-exposed
894 atoms from residues that are not always sequential, while LBL epitopes are made up of
895 sequential residues. Antibodies that identify LBL epitopes can recognize denatured antigens,
896 but denaturing the antigen causes conformational B-cell epitopes to lose their recognition
897 [144]. T-cell and B-cell epitopes have been predicted for the selected RSV proteins using the
898 IEDB server. The most conserved epitopes with high antigenicity, non-allergenicity, and non-
899 toxicity were screened for designing the vaccine construct. The broad-spectrum activity of the
900 vaccine over the selected strains of both RSV-A and RSV-B viruses was assured by the
901 conservancy of the epitopes.

902 Furthermore, the cytokine-producing ability was considered as a criterion to screen the HTL
903 epitopes desired for designing the vaccine. Inflammatory mediators, such as cytokines and
904 chemokines have been linked to RSV pathogenesis. They may be divided into two groups
905 depending on how they affect immune cells: pro-inflammatory and anti-inflammatory
906 chemicals [144]. Interleukin (IL)-1, tumor necrosis factor-alpha (TNF-α), interferon-gamma
907 (IFN- γ), and interleukin-6 (IL-6) are pro-inflammatory cytokines [145-147]. IL-10 and IL-12
908 are anti-inflammatory cytokines [148, 149]. IFN-γ , on the other hand, has a dual role during
909 RSV infection; it is essential to decrease viral multiplication while simultaneously inhibiting
910 airway blockage [150]. IFN-γ is well-known for its fundamentally safe responses and potential
911 to stop viral multiplication [151, 152]. Additionally, IL-4 plays important role in regulating the
912 responses of lymphocytes, myeloid cells, and non-hematopoietic cells. In T-cells, IL-4 induces
913 the differentiation of naïve CD4 T cells into Th2 cells, and in B cells, IL-4 drives the
914 immunoglobulin (Ig) class switch to IgG1 and IgE, and in macrophages, IL-4, as well as IL-
915 13, induce alternative macrophage activations [153]. Consequently, cytokines including IFN-
916 γ, IL-10, and IL-4 were considered essential during the prediction of the HTL epitopes of the
917 vaccine which, after administration, might play a crucial role in creating a network between
918 immune system cells [63]. The population coverage analysis was performed in the following
919 step. As HLA allelic distribution varies between geographical regions and ethnic groups
920 throughout the world, it is paramount to consider population coverage while designing a viable
921 epitope-based vaccine that is pertinent to global populations. According to the population
922 coverage analysis, the MHC Class-I and Class-II alleles and their epitopes covered 85.70 %
923 and 87.92 % of the global population, respectively, while the combined MHC Class-I and class-
924 II alleles and their epitopes covered 84% of the world population. When compared to the
925 overall population, selected epitopes exhibited a greater individual percentage cover which
926 indicates the potential worldwide effects of the vaccine against RSV infections.

927

928 The most promising epitopes had been conjugated by specific linkers, i.e. EAAAK, AAY, KK,
929 and GPGPG. An innate antimicrobial peptide, hBD-3 was used as an adjuvant during the
930 construction of the vaccine. An adjuvant is considered crucial for designing a subunit vaccine
931 because it improves the traits of antigenicity, immunogenicity, durability, and longevity of the
932 subunit vaccine [154]. The hBD-3 was chosen as it could potentially induce TLR-dependent
933 expression of the co-stimulatory molecules - CD80, CD86, and CD40 on the surface of
934 monocytes and myeloid dendritic cells [155]. Moreover, by forming a protective barrier of
935 immobilized surface proteins, hBD-3 can prevent the fusion of the virus [156]. Furthermore, it
936 activates the APCs through TLR1 and TLR2 [157], stimulates IL-22 [158], TGF-α [159, 160],
937 and IFN-γ [161, 162]. It also facilitates the chemotaxis of immature DCs and T cells through
938 its interaction with chemokine receptor 6 (CCR6), as well as the chemotaxis of monocytes
939 through its interaction with CCR2 [163]. This peptide also promotes and activates myeloid
940 DCs and natural killer (NK) cells [157, 162].

941 Alongside the adjuvant, to strengthen the immunogenic reaction of the vaccine, the PADRE
942 sequence was also incorporated. The antigenicity, allergenicity, and physicochemical
943 properties of the constructed vaccine were subsequently identified, which revealed the vaccine
944 protein to be desirable for further modeling refinement and validation processes. The vaccine
945 protein was predicted with a theoretical pI of 9.75, indicating that the vaccine protein is basic
946 and it might belong to the positively charged proteins [132]. The vaccine's GRAVY value was
947 predicted to be quite negative (-0.362), indicating that the vaccine protein is hydrophilic [138,
948 139]. Moreover, the instability index was determined to be less than 40 (27.55), implying that
949 the vaccine is fairly stable. The extinction coefficient which is representative of the light-
950 absorbing nature, and the aliphatic index which denotes the high stability of the vaccine protein,
951 were both found to have high values at 45770 M-1 cm-1 and 80.85, respectively [133]. Using

different online tools to predict the secondary and tertiary structure of the vaccine, it was revealed that the adjuvant sequences had produced some substantial changes in the predicted vaccine construct. Furthermore, the secondary structure analysis showed that the vaccine protein sequence was abundant with the coiled regions as well as the very low amount of β-strand. This indicates the higher stability and conservation of the predicted vaccine model. The tertiary structure was modeled and refined once the secondary structure was determined. The tertiary structure prediction of the vaccine protein revealed a p-value of 8.71e-05 in four domains of the protein, indicating that the predicted 3D structure was quite accurate. The quality of the vaccine was greatly enhanced following refinement in the context of GDT-HA, MolProbity, Rama favored amino acid percentage, and z scores, according to the tertiary structure refinement and validation study. With only a few amino acids in the outlier regions, the refined structure showed a very high Rama favored amino acid percentage. Following that, the refined structure was used for disulfide engineering. Furthermore, disulfide engineering of the vaccine construct has been conducted to increase its stability using the DbD2 v12.2 servers. The server can determine the B-factor of areas involved in disulfide bonding as well as identify potential disulfides that increase the protein's thermal stability [92]. All residue pairings in a given protein structural model are quickly analyzed for closeness and geometry compatible with disulfide formation, assuming the residues have been changed to cysteines. Similarly, the experimental result shows residue pairings that match the specified requirements. Engineered disulfides have been shown to improve protein stability and aid in the study of protein dynamics and interactions [94]. Three pairs of amino acids have been found by the server which is predicted to improve the stability of the vaccine construct thereby. However, the vaccine's possible effectiveness and immunological responses may be reduced if posttranslational modification, such as glycosylation and phosphorylation, is overlooked during vaccine development. Glycosylation is a chemical modification of macromolecules in which

977 carbohydrate moieties are covalently bonded to the N or C terminals of lipids and proteins
978 molecules, resulting in N-linked and O-linked glycosylation [164]. Previous studies have found
979 that glycosylation significantly improves vaccine immunogenicity when compared to non-
980 glycosylated vaccinations, and clinical trials are now ongoing [165]. Furthermore,
981 phosphorylation is the process of adding a phosphate group to macromolecules. Eukaryotes
982 have a greater frequency of occurrence of posttranslational modifications. Serine and threonine
983 are two important phosphorylation sites. Phosphorylated peptides or epitopes (synthetic or
984 natural) are known to be better recognized by cytotoxic T cells, i.e. MHC Class I molecules,
985 and are therefore directly implicated in the production of particular immune responses [166].
986 As a result, it is hypothesized that the vaccine construct predicted with multiple
987 posttranslational modifications will create an efficient immunogenic response against the virus
988 following vaccine administration.

989 Furthermore, one of the predominant necessities and approaches to designing an effective
990 vaccine is the molecular docking process. It concludes the probability of contact between the
991 vaccine and other networking proteins, i.e. TLRs may occur during initial immune response.
992 TLRs, which are found on leukocytes and in tissues, play a major role in innate immunity
993 activation by identifying invading pathogens, including viruses like RSV, and sending out
994 signals that promote inflammation-related components [167]. TLRs, such as TLR2, TLR1,
995 TLR6, TLR3, and TLR4, are found on leukocytes and can interact with RSV to boost immune
996 responses [168]. Within the lungs, TLR2 interactions with RSV increase neutrophil migration
997 and dendritic cell activation. TLR2 exists as a heterodimer complex with either TLR1 or TLR6
998 on the surface of immune cells and tissues [169]. According to genetic analysis and vaccine
999 studies, TLR2 signaling appears to be critical in RSV recognition [170-172]. TLR2 and TLR1
1000 or TLR2 and TLR6 complexes can recognize RSV, and greatly enhance early innate
1001 inflammatory responses [173-175]. Previous research has also suggested that the signals

generated by TLR2 and TLR6 activation are critical for viral replication control [168]. TLR3 and TLR4 signaling support the T helper type 1 (Th1) responses, whereas T helper type 2 (Th2) responses are favored by TLR2/1, and TLR2/6 signaling [177]. Th1 cells help with responses to intracellular pathogens, whereas Th2 cells handle parasitic infections and allergies [178, 179]. The F glycoprotein of RSV has been reported to induce primarily a Th1-type immune response through the interaction with TLR4 [180, 181]. On the other hand, TLR9 has been found to improve vaccine immunogenicity and decrease vaccine-enhanced illness during FI-RSV immunization. Furthermore, immunomodulation generated by TLR9 agonists verifies TLR agonists' adjuvant potential after RSV immunization [182]. Finally, the targeted TLRs are all involved in pattern recognition and the innate immune response to RSV, which results in the production of proinflammatory cytokines and chemokines [183]. TLRs which are critical in the RSV pathogenesis were considered for the docking analysis. Thus, TLR-1, TLR-2, TLR-3, TLR-4, and TLR9 have been docked with the vaccine protein which revealed each of the TLRs to obtain very low binding energy in different servers and to show strong interaction with the vaccine protein according to the results given in the docking analysis. It is evident from the docking analysis that the designed vaccine would have a strong affinity with all the target TLRs, leading to the possibility that a strong immune response might be induced by the vaccine after administration.

In response to external forces exerted by its surrounding environment, MD simulation examines the motion and changes in the state of a target protein molecule or complex. In this experiment, to get a better insight into their molecular stability, the five docked vaccine-TLR complexes were simulated. The experiment revealed that the structures retained appropriate levels of deviation. The TLR1-vaccine complex was found to have the least RMSD compared to other complexes; the TLR4-vaccine complex had higher RMSD despite having a similar number of chains. The result of RMSD represents the stability of TLR1 and TLR9 vaccine

complexes. Despite 3 chains *viz.* Chain A, chain B, and vaccine chain in the TLR1-vaccine complex, the resultant RMSD, suggest reasonable stability. Furthermore, The RMSF analysis suggests the residues in the range 190-240 and 480-530 are having large magnitudes of fluctuations in all the complexes. The TLR3-vaccine complex showed slightly larger fluctuating side chains than other complexes. The results of the total Rg analysis suggest that the total Rg of the TLR1-vaccine complex almost remained constant throughout the simulation. The total Rg of the TLR4-vaccine complex was found lower; however, it deviated throughout the simulation. Though both these TLRs have two chains of proteins along with vaccine chains, TLR1 Rg seemed quite stable, while the other TLR systems (TLR2, TLR3) also seemed to be quite compact, and there were no evident secondary structural changes in these TLRs. In the non-bonded interaction analysis, in the case of TLR1-vaccine complex, it is found that around 10 hydrogen bonds were formed till around 50 ns MD time interval, which steadily lowers to around 5 hydrogen bonds till 80 ns and thereafter rises to 10 hydrogen bonds. The TLR2-vaccine complex has around 7 hydrogen bonds being constantly formed throughout the MD simulation, while TLR3 and TLR9 complexes with vaccines have around 10 hydrogen bonds constantly formed. These complexes have strong hydrogen bond networks at the interface of TLRs and vaccines. The TLR4-vaccine complex has around 5 hydrogen bonds formed which are fewer in number compared to other systems. Actual residues involved in the hydrogen bond formation as investigated in the last trajectory are tabulated in the **S7 Table.**

The immune simulation analysis of the proposed vaccine demonstrated that the vaccine could induce an immune response compatible with the natural host immune system. Both humoral and cell-mediated responses may be activated by the vaccine, as shown by an elevation in the levels of memory B cells, plasma B cells, cytotoxic T cells, helper T cells, and various antibodies. Adaptive immunity is an immunity that occurs after exposure to an antigen either

from a pathogen or a vaccination. A vaccine can generate adaptive immunity against the pathogen by which it may restrict or prevent the infection. The vaccine-provided activation of helper T cells resulted in strong adaptive immunity [184-186]. Again, a very strong antigen presentation was also demonstrated in the simulation study by the rise in the concentration of APCs such as macrophages and dendritic cells. In addition, enrichment in the cytokine profile that plays a crucial role in providing broad-spectrum immunity against viral invasions [186-189] has also been identified in the analysis [66]. Moreover, the gradual increase in the level of different mucosal immunoglobulins i.e. IgG1 + IgG2, and IgG + IgM antibodies throughout the vaccine doses or injections were also predicted. The mucosal immune system is the dominant part of the immune system, having developed to protect the mucosae in the upper respiratory tract, which are the primary sites of respiratory infection. Being a respiratory virus, RSV initially affects the upper respiratory tract, due to which the immune system may be stimulated against the virus predominantly at the mucosal surfaces [190]. Previous clinical studies also reported IgG and IgM to be significant role players against RSV infections [191]. Furthermore, the simulation analysis revealed that the concentration of regulatory T cells would gradually decrease throughout the phases of the vaccine doses which indicates the potential decrease in suppression of vaccine-induced immunity by regulatory T cells [192].

Hence, the proposed vaccine construct is predicted to produce an effective immunogenic response after the vaccine injections, according to the analysis of the immune simulation. The codon adaptation and subsequent *in silico* cloning studies were conducted to identify the potential codons required for the generation of a recombinant plasmid that could be used to express the vaccine in the *E. coli* strain K12, leading to the mass manufacturing efforts of the vaccine in the near future. The *E.coli* cell culture system is considered to be the majorly recommended system for the production of recombinant proteins at a mass level. In the codon adaptation analysis, the obtained results were significantly good with a CAI value of 0.98 and

a GC content of 50.23 %, since any CAI value above 0.80 and a GC content of 30% to 70% are considered to be the most promising scores [34, 186, 193]. Following this, the optimized vaccine DNA sequence was inserted into the pETite plasmid vector using Snapgene restriction cloning software. The pETite plasmid vector contains SUMO tag and 6X His tag which might be fused with the vaccine codon sequence during the *in silico* cloning process. This may lead to the expression of these tags within the protein itself, which could promote the purification and downstream processing of the vaccine. Prediction of the stability of the vaccine mRNA secondary structure using the Mfold and RNAfold servers provided with the negative and much lower minimal free energies of -549.30 and -526.30 kcal/mol, respectively. The lower minimal free energy is often considered better than the higher maximal free energy score which indicates the protein to be more stable. It can, therefore, be reported that the predicted vaccine could be very stable upon transcription [133]. Overall, this study suggests that the proposed vaccine peptide could be utilized as a potential and successful protective measure against both RSV-A and RSV-B subtypes. However, to eventually validate its immunogenicity, efficacy, stability, safety, and various biophysical characteristics, further research approaches, and implementations are recommended.

5. Conclusion

RSV is predominantly one of the major contributors of diseases of the LRTI, including pneumonia and bronchiolitis, responsible for infecting people of all ages as well as immunocompromised individuals with a high infection rate. Millions of individuals eventually end up being diagnosed with this virus every year, and a huge proportion of them require to be hospitalized. While research for an effective countermeasure to tackle this virus has been ongoing for the past few decades, no approved vaccine is still commercially available.

Moreover, the antiviral drugs now available often struggle to show any effective outcomes during therapy. Therefore, a potential epitope-based polyvalent vaccine against both forms of RSV, RSV-A, and RSV-B, was designed in this research using the techniques of immunoinformatics and *in-silico* biology. The vaccine included the T-cell and B-cell epitopes that were 100% conserved; they could therefore be efficient against the two selected viruses. In addition, high antigenicity, non-allergenicity, and non-toxicity as well as non-homology (to the human proteome) were also considered to be the criteria for choosing the most promising epitopes for the final construction of the vaccine, so that the vaccine could deliver a very strong immunogenic response without triggering any adverse reaction inside the body. The results of the various analyses conducted in the study revealed that the polyvalent vaccine should be very safe, efficient, and responsive to use. The tools utilized in this study are well accepted and yield highly accurate results. Therefore, the findings of this study can point researchers in the direction of novel vaccine development tactics. Researchers could investigate the predicted epitopes and their probable immunogenic response elicited in the host system when looking into further subunit vaccine development or other prevention strategies against RSV infection. However, as all these predictions were focused solely on computational techniques, it is important to perform further wet laboratory-based experiments to validate the findings of this analysis. With high-cost criteria and numerous drawbacks in improving the preparation of a live, attenuated, or inactivated vaccine for such highly infectious agents, candidates for peptide-based vaccines, such as the one designed in this study, maybe comparatively cheap and an efficient alternative to reach the entire world as a polyvalent vaccine to fight the challenge of RSV infections.

6. Acknowledgements

Authors are thankful to the Department of Pharmaceutical Chemistry, Sinhgad College of Pharmacy, Maharashtra, India, Department of Genetic Engineering and Biotechnology,

University of Chittagong, Chattogram, Bangladesh and Swift Integrity Computational Lab, Dhaka, Bangladesh, a virtual platform of young researchers, for providing support to successfully carry out the research.

7. Declarations

Ethics approval and consent to participate

Not Applicable

Consent for publication

Not Applicable

Availability of data and material

All the data generated during the experiment are provided in the manuscript/supplementary material.

Competing interests

The authors declare that they have no conflict of interest regarding the publication of the paper.

Funding

No funding was received from any external sources.

8. References

1. Meng J, Stobart CC, Hotard AL, Moore ML. An overview of respiratory syncytial virus. PLoS Pathog. 2014 Apr 24;10(4):e1004016.
https://doi.org/10.1371/journal.ppat.1004016
PMid:24763387 PMCid:PMC3999198

2. Clark CM, Guerrero-Plata A. Respiratory syncytial virus vaccine approaches: a current overview. Current clinical microbiology reports. 2017 Dec 1;4(4):202-7
https://doi.org/10.1007/s40588-017-0074-6
PMid:30009126 PMCid:PMC6040676

3. Killikelly A, Tunis M, House A, Quach C, Vaudry W, Moore D. Respiratory syncytial virus: Overview of the respiratory syncytial virus vaccine candidate pipeline in Canada. Canada Communicable Disease Report. 2020 Apr 2;46(4):56
https://doi.org/10.14745/ccdr.v46i04a01
PMid:32510521 PMCid:PMC7273503

4. Schmidt ME, Varga SM. Modulation of the host immune response by respiratory syncytial virus proteins. Journal of Microbiology. 2017 Mar 1;55(3):161-71.
https://doi.org/10.1007/s12275-017-7045-8
PMid:28243940

5. Bakre AA, Harcourt JL, Haynes LM, Anderson LJ, Tripp RA. The central conserved region (CCR) of respiratory syncytial virus (RSV) G protein modulates host miRNA expression and alters the cellular response to infection. Vaccines. 2017 Sep;5(3):16.
https://doi.org/10.3390/vaccines5030016
PMid:28671606 PMCid:PMC5620547

6. Harcourt J, Alvarez R, Jones LP, Henderson C, Anderson LJ, Tripp RA. Respiratory syncytial virus G protein and G protein CX3C motif adversely affect CX3CR1+ T cell responses. The Journal of Immunology. 2006 Feb 1;176(3):1600-8.
https://doi.org/10.4049/jimmunol.176.3.1600
PMid:16424189

7. Bergeron HC, Murray J, Castrejon AM, DuBois RM, Tripp RA. Respiratory Syncytial Virus (RSV) G Protein Vaccines With Central Conserved Domain Mutations Induce CX3C-CX3CR1 Blocking Antibodies. Viruses. 2021 Feb;13(2):352.
https://doi.org/10.3390/v13020352
PMid:33672319 PMCid:PMC7926521

8. Eshaghi A, Duvvuri VR, Lai R, Nadarajah JT, Li A, Patel SN, Low DE, Gubbay JB. Genetic variability of human respiratory syncytial virus A strains circulating in Ontario: a novel genotype with a 72 nucleotide G gene duplication. PloS one. 2012 Mar 28;7(3):e32807.
https://doi.org/10.1371/journal.pone.0032807
PMid:22470426 PMCid:PMC3314658

9. Yoshihara K, Le MN, Okamoto M, Wadagni AC, Nguyen HA, Toizumi M, Pham E, Suzuki M, Nguyen AT, Oshitani H, Ariyoshi K. Association of RSV-A ON1 genotype with increased pediatric acute lower respiratory tract infection in Vietnam. Scientific Reports. 2016 Jun 16;6(1):1-0.
https://doi.org/10.1038/srep27856
PMid:27306333 PMCid:PMC4910061

10. Chirkova T, Boyoglu-Barnum S, Gaston KA, Malik FM, Trau SP, Oomens AG, Anderson LJ. Respiratory syncytial virus G protein CX3C motif impairs human airway epithelial and immune cell responses. Journal of virology. 2013 Dec 15;87(24):13466-79.
https://doi.org/10.1128/JVI.01741-13
PMid:24089561 PMCid:PMC3838285

11. Resch B. Product review on the monoclonal antibody palivizumab for prevention of respiratory syncytial virus infection. Human vaccines & immunotherapeutics. 2017 Sep 2;13(9):2138-49.
https://doi.org/10.1080/21645515.2017.1337614
PMid:28605249 PMCid:PMC5612471

12. IMpact-RSV Study Group*. Palivizumab, a humanized respiratory syncytial virus monoclonal antibody, reduces hospitalization from respiratory syncytial virus infection in high-risk infants. Pediatrics. 1998 Sep 1;102(3):531-7.
https://doi.org/10.1542/peds.102.3.531

13. Bergeron HC, Tripp RA. Emerging small and large molecule therapeutics for respiratory syncytial virus. Expert opinion on investigational drugs. 2020 Mar 3;29(3):285-94.
https://doi.org/10.1080/13543784.2020.1735349
PMid:32096420

14. Bianchini S, Silvestri E, Argentiero A, Fainardi V, Pisi G, Esposito S. Role of Respiratory Syncytial Virus in Pediatric Pneumonia. Microorganisms. 2020 Dec;8(12):2048.
https://doi.org/10.3390/microorganisms8122048
PMid:33371276 PMCid:PMC7766387

15. Falsey AR, Walsh EE. Respiratory syncytial virus infection in elderly adults. Drugs & aging. 2005 Jul;22(7):577-87.
https://doi.org/10.2165/00002512-200522070-00004
PMid:16038573 PMCid:PMC7099998

16. Agoti CN, Phan MV, Munywoki PK, Githinji G, Medley GF, Cane PA, Kellam P, Cotten M, Nokes DJ. Genomic analysis of respiratory syncytial virus infections in households and utility in inferring who infects the infant. Scientific reports. 2019 Jul 11;9(1):1-4
https://doi.org/10.1038/s41598-019-46509-w
PMid:31296922 PMCid:PMC6624209

17. Kim HW, Canchola JG, Brandt CD, Pyles G, Chanock RM, Jensen K, Parrott RH. Respiratory syncytial virus disease in infants despite prior administration of antigenic inactivated vaccine. American journal of epidemiology. 1969 Apr 1;89(4):422-34.
https://doi.org/10.1093/oxfordjournals.aje.a120955
PMid:4305198

18. Fulginiti VA, Eller JJ, Sieber OF, Joyner JW, Minamitani M, Meiklejohn G. Respiratory virus immunization: A field trial of two inactivated respiratory virus vaccines; an aqueous trivalent paratnfluenza virus vaccine and an alum-precipitated Respiratory Syncytial Virus vaccine. American journal of epidemiology. 1969 Apr 1;89(4):435-48.
https://doi.org/10.1093/oxfordjournals.aje.a120956
PMid:4305199

19. CHIN J, MAGOFFIN RL, SHEARER LA, SCHIEBLE JH, LENNETTE EH. Field evaluation of a respiratory syncytial virus vaccine and a trivalent parainfluenza virus vaccine in a pediatric population. American journal of epidemiology. 1969 Apr 1;89(4):449-63.
https://doi.org/10.1093/oxfordjournals.aje.a120957
PMid:4305200

20. Kapikian AZ, Mitchell RH, Chanock RM, Shvedoff RA, Stewart CE. An epidemiologic study of altered clinical reactivity to respiratory syncytial (RS) virus infection in children previously vaccinated with an inactivated RS virus vaccine. American journal of epidemiology. 1969 Apr 1;89(4):405-21.
https://doi.org/10.1093/oxfordjournals.aje.a120954
PMid:4305197

21. Kim HW, Arrobio JO, Pyles G, Brandt CD, Camargo E, Chanock RM, Parrott RH. Clinical and immunological response of infants and children to administration of low-temperature adapted respiratory syncytial virus. Pediatrics. 1971 Nov 1;48(5):745-55.
https://doi.org/10.1542/peds.48.5.745
PMid:4330595

22. Olson MR, Varga SM. CD8 T cells inhibit respiratory syncytial virus (RSV) vaccine-enhanced disease. The Journal of Immunology. 2007 Oct 15;179(8):5415-24.
https://doi.org/10.4049/jimmunol.179.8.5415
PMid:17911628

23. Olson MR, Hartwig SM, Varga SM. The number of respiratory syncytial virus (RSV)-specific memory CD8 T cells in the lung is critical for their ability to inhibit RSV vaccine-enhanced pulmonary eosinophilia. The Journal of Immunology. 2008 Dec 1;181(11):7958-68.
https://doi.org/10.4049/jimmunol.181.11.7958
PMid:19017987 PMCid:PMC2587004

24. Knudson CJ, Hartwig SM, Meyerholz DK, Varga SM. RSV vaccine-enhanced disease is orchestrated by the combined actions of distinct CD4 T cell subsets. PLoS pathogens. 2015 Mar 13;11(3):e1004757.
https://doi.org/10.1371/journal.ppat.1004757
PMid:25769044 PMCid:PMC4358888

25. Delgado MF, Coviello S, Monsalvo AC, Melendi GA, Hernandez JZ, Batalle JP, Diaz L, Trento A, Chang HY, Mitzner W, Ravetch J. Lack of antibody affinity maturation due to poor Toll-like receptor stimulation leads to enhanced respiratory syncytial virus disease. Nature medicine. 2009 Jan;15(1):34-41.
https://doi.org/10.1038/nm.1894
PMid:19079256 PMCid:PMC2987729

26. Karron RA, Wright PF, Crowe Jr JE, Mann ML, Thompson J, Makhene M, Casey R, Murphy BR. Evaluation of two live, cold-passaged, temperature-sensitive respiratory syncytial virus vaccines in chimpanzees and in human adults, infants, and children. Journal of Infectious Diseases. 1997 Dec 1;176(6):1428-36.
https://doi.org/10.1086/514138
PMid:9395351

27. Gomez M, Mufson MA, Dubovsky F, Knightly C, Zeng W, Losonsky G. Phase-I study MEDI-534, of a live, attenuated intranasal vaccine against respiratory syncytial virus and parainfluenza-3 virus in seropositive children. The Pediatric infectious disease journal. 2009 Jul 1;28(7):655-8.
https://doi.org/10.1097/INF.0b013e318199c3b1
PMid:19483659

28. Ascough S, Vlachantoni I, Kalyan M, Haijema BJ, Wallin-Weber S, Dijkstra-Tiekstra M, Ahmed MS, Van Roosmalen M, Grimaldi R, Zhang Q, Leenhouts K. Local and systemic immunity against respiratory syncytial virus induced by a novel intranasal vaccine. A randomized, double-blind, placebo-controlled clinical trial. American journal of respiratory and critical care medicine. 2019 Aug 15;200(4):481-92.
https://doi.org/10.1164/rccm.201810-1921OC
PMid:30753101 PMCid:PMC6701032

29. Shafique M, Zahoor MA, Arshad MI, Aslam B, Siddique AB, Rasool MH, Qamar MU, Usman M. Hurdles in Vaccine Development against Respiratory Syncytial Virus. InThe Burden of Respiratory Syncytial Virus Infection in the Young 2019 Aug 1. IntechOpen.
https://doi.org/10.5772/intechopen.87126

30. Xing Y, Proesmans M. New therapies for acute RSV infections: where are we?. European journal of pediatrics. 2019 Feb 12;178(2):131-8.
https://doi.org/10.1007/s00431-018-03310-7
PMid:30610420

31. Griffiths C, Drews SJ, Marchant DJ. Respiratory syncytial virus: infection, detection, and new options for prevention and treatment. Clinical microbiology reviews. 2017 Jan 1;30(1):277-319.
https://doi.org/10.1128/CMR.00010-16
PMid:27903593 PMCid:PMC5217795

32. Jordan R, Shao M, Mackman RL, Perron M, Cihlar T, Lewis SA, Eisenberg EJ, Carey A, Strickley RG, Chien JW, Anderson ML. Antiviral efficacy of a respiratory syncytial virus (RSV) fusion inhibitor in a bovine model of RSV infection. Antimicrobial agents and chemotherapy. 2015 Aug 1;59(8):4889-900
https://doi.org/10.1128/AAC.00487-15
PMid:26055364 PMCid:PMC4505261

33. María, R.R., Arturo, C.J., Alicia, J.A., Paulina, M.G., Gerardo, A.O., 2017. The impact of bioinformatics on vaccine design and development. InTech, Rijeka, Croatia.
https://doi.org/10.5772/intechopen.69273

34. Sarkar B, Ullah MA, Araf Y, Das S, Hosen MJ. Blueprint of epitope-based multivalent and multipathogenic vaccines: targeted against the dengue and zika viruses. Journal of Biomolecular Structure and Dynamics. 2020a Aug 7:1-21.
https://doi.org/10.1080/07391102.2020.1804456
PMid:32772811

35. Rappuoli R. Reverse vaccinology. Current opinion in microbiology. 2000 Oct 1;3(5):445-50.
https://doi.org/10.1016/S1369-5274(00)00119-3

36. Rappuoli, R., Bottomley, M.J., D'Oro, U., Finco, O., De Gregorio, E., 2016. Reverse vaccinology 2.0: Human immunology instructs vaccine antigen design. J. Exp. Med. 213, 469-481.
https://doi.org/10.1084/jem.20151960
PMid:27022144 PMCid:PMC4821650

37. Chong, L.C. and Khan, A.M., 2019. Vaccine Target Discovery.
https://doi.org/10.1016/B978-0-12-809633-8.20100-3
PMCid:PMC7148608

38. Collins PL, Fearns R, Graham BS. Respiratory syncytial virus: virology, reverse genetics, and pathogenesis of disease. InChallenges and opportunities for respiratory syncytial virus vaccines 2013 (pp. 3-38). Springer, Berlin, Heidelberg.
https://doi.org/10.1007/978-3-642-38919-1_1
PMid:24362682 PMCid:PMC4794264

39. Steff AM, Monroe J, Friedrich K, Chandramouli S, Nguyen TL, Tian S, Vandepaer S, Toussaint JF, Carfi A. Pre-fusion RSV F strongly boosts pre-fusion specific neutralizing responses in cattle pre-exposed to bovine RSV. Nature communications. 2017 Oct 20;8(1):1-0.
https://doi.org/10.1038/s41467-017-01092-4
PMid:29057917 PMCid:PMC5651886

40. McLellan JS, Ray WC, Peeples ME. Structure and function of respiratory syncytial virus surface glycoproteins. Challenges and opportunities for respiratory syncytial virus vaccines. 2013:83-104.
https://doi.org/10.1007/978-3-642-38919-1_4
PMid:24362685 PMCid:PMC4211642

41. Arbiza J, Taylor G, López JA, Furze J, Wyld S, Whyte P, Stott EJ, Wertz G, Sullender W, Trudel M, Melero JA. Characterization of two antigenic sites recognized by neutralizing monoclonal antibodies directed against the fusion glycoprotein of human respiratory syncytial virus. Journal of General Virology. 1992 Sep 1;73(9):2225-34.
https://doi.org/10.1099/0022-1317-73-9-2225
PMid:1383404

42. Lopez JA, Bustos R, Örvell C, Berois M, Arbiza J, García-Barreno B, Melero JA. Antigenic structure of human respiratory syncytial virus fusion glycoprotein. Journal of virology. 1998 Aug 1;72(8):6922-8.
https://doi.org/10.1128/JVI.72.8.6922-6928.1998
PMid:9658147 PMCid:PMC109907

43. López JA, Peñas CO, García-Barreno BL, Melero JA, Portela A. Location of a highly conserved neutralizing epitope in the F glycoprotein of human respiratory syncytial virus. Journal of virology. 1990 Feb;64(2):927-30.
https://doi.org/10.1128/jvi.64.2.927-930.1990
PMid:1688629 PMCid:PMC249192

44. Lu B, Ma CH, Brazas R, Jin H. The major phosphorylation sites of the respiratory syncytial virus phosphoprotein are dispensable for virus replication in vitro. Journal of virology. 2002 Nov 1;76(21):10776-84
https://doi.org/10.1128/JVI.76.21.10776-10784.2002
PMid:12368320 PMCid:PMC136636

45. Doytchinova, I.A., Flower, D.R., 2007. VaxiJen: a server for prediction of protective antigens, tumour antigens and subunit vaccines. BMC Bioinform. 8, 4.
https://doi.org/10.1186/1471-2105-8-4
PMid:17207271 PMCid:PMC1780059

46. Gasteiger, E., Hoogland, C., Gattiker, A., Wilkins, M.R., Appel, R.D. and Bairoch, A., 2005. Protein identification and analysis tools on the ExPASy server. In The proteomics protocols handbook (pp. 571-607). Humana press.

https://doi.org/10.1385/1-59259-890-0:571

47. Clem AS. Fundamentals of vaccine immunology. Journal of global infectious diseases. 2011 Jan;3(1):73.
https://doi.org/10.4103/0974-777X.77299
PMid:21572612 PMCid:PMC3068582

48. Chaudhri, G., Quah, B.J., Wang, Y., Tan, A.H., Zhou, J., Karupiah, G. and Parish, C.R., 2009. T cell receptor sharing by cytotoxic T lymphocytes facilitates efficient virus control. Proceedings of the National Academy of Sciences, 106(35), pp.14984-14989.
https://doi.org/10.1073/pnas.0906554106
PMid:19706459 PMCid:PMC2736460

49. Zhu, J. and Paul, W.E., 2008. CD4 T cells: fates, functions, and faults. Blood, The Journal of the American Society of Hematology, 112(5), pp.1557-1569.
https://doi.org/10.1182/blood-2008-05-078154
PMid:18725574 PMCid:PMC2518872

50. Cooper, N.R. and Nemerow, G.R., 1984. The role of antibody and complement in the control of viral infections. Journal of investigative dermatology, 83(s 1), pp.121-127.
https://doi.org/10.1038/jid.1984.33

51. Sun P, Ju H, Liu Z, Ning Q, Zhang J, Zhao X, Huang Y, Ma Z, Li Y. Bioinformatics resources and tools for conformational B-cell epitope prediction. Computational and mathematical methods in medicine. 2013 Jul 21;2013.
https://doi.org/10.1155/2013/943636
PMid:23970944 PMCid:PMC3736542

52. Zhang J, Zhao X, Sun P, Gao B, Ma Z. Conformational B-cell epitopes prediction from sequences using cost-sensitive ensemble classifiers and spatial clustering. BioMed research international. 2014 Jun 17;2014.
https://doi.org/10.1155/2014/689219
PMid:25045691 PMCid:PMC4083607

53. Vita R, Mahajan S, Overton JA, Dhanda SK, Martini S, Cantrell JR, Wheeler DK, Sette A, Peters B. The Immune Epitope Database (IEDB): 2018 update. Nucleic Acids Res. 2018 Oct 24.
https://doi.org/10.1093/nar/gky1006
PMid:30357391 PMCid:PMC6324067

54. Jespersen MC, Peters B, Nielsen M, Marcatili P. BepiPred-2.0: improving sequence-based B-cell epitope prediction using conformational epitopes. Nucleic acids research. 2017 Jul 3;45(W1):W24-9.
https://doi.org/10.1093/nar/gkx346

PMid:28472356 PMCid:PMC5570230

55. Gruber AR, Lorenz R, Bernhart SH, Neuböck R, Hofacker IL. The vienna RNA websuite. Nucleic acids research. 2008 Apr 19;36(suppl_2):W70-4.
https://doi.org/10.1093/nar/gkn188
PMid:18424795 PMCid:PMC2447809

56. Ponomarenko J, Bui HH, Li W, Fusseder N, Bourne PE, Sette A, Peters B. ElliPro: a new structure-based tool for the prediction of antibody epitopes. BMC bioinformatics. 2008 Dec;9(1):1-8.
https://doi.org/10.1186/1471-2105-9-514
PMid:19055730 PMCid:PMC2607291

57. Bibi S, Ullah I, Zhu B, Adnan M, Liaqat R, Kong WB, Niu S. In silico analysis of epitope-based vaccine candidate against tuberculosis using reverse vaccinology. Scientific Reports. 2021 Jan 13;11(1):1-6.
https://doi.org/10.1038/s41598-020-80899-6
PMid:33441913 PMCid:PMC7807040

58. Bui HH, Sidney J, Li W, Fusseder N, Sette A. Development of an epitope conservancy analysis tool to facilitate the design of epitope-based diagnostics and vaccines. BMC bioinformatics. 2007 Dec 1;8(1):361.
https://doi.org/10.1186/1471-2105-8-361
PMid:17897458 PMCid:PMC2233646

59. Dimitrov, I., Flower, D.R. and Doytchinova, I., 2013, April. AllerTOP-a server for in-silico prediction of allergens. In BMC bioinformatics (Vol. 14, No. 6, p. S4). BioMed Central.
https://doi.org/10.1186/1471-2105-14-S6-S4
PMid:23735058 PMCid:PMC3633022

60. Dimitrov, I., Naneva, L., Doytchinova, I. and Bangov, I., 2014. AllergenFP: allergenicity prediction by descriptor fingerprints. Bioinformatics, 30(6), pp.846-851.
https://doi.org/10.1093/bioinformatics/btt619
PMid:24167156

61. Gupta, S., Kapoor, P., Chaudhary, K., Gautam, A. and Kumar, R., 2013. Consortium, OSDD; Raghava, GPS In-silico Approach for Predicting Toxicity of Peptides and Proteins. PLoS One, 8, p.e73957
https://doi.org/10.1371/journal.pone.0073957
PMid:24058508 PMCid:PMC3772798

62. Krogh, A., Larsson, B., Von Heijne, G., & Sonnhammer, E. L. (2001). Predicting transmembrane protein topology with a hidden Markov model: Application to complete genomes. Journal of Molecular Biology, 305(3), 567-580.
https://doi.org/10.1006/jmbi.2000.4315
PMid:11152613

63. Luckheeram, R.V., Zhou, R., Verma, A.D. and Xia, B., 2012. CD4+ T cells: differentiation and functions. Clinical and developmental immunology, 2012.
https://doi.org/10.1155/2012/925135
PMid:22474485 PMCid:PMC3312336

64. Dhanda SK, Gupta S, Vir P, Raghava GP. Prediction of IL4 inducing peptides. Clinical and Developmental Immunology. 2013 Oct;2013.
https://doi.org/10.1155/2013/263952
PMid:24489573 PMCid:PMC3893860

65. Dhanda SK, Vir P, Raghava GP. Designing of interferon-gamma inducing MHC class-II binders. Biology direct. 2013 Dec;8(1):30.
https://doi.org/10.1186/1745-6150-8-30
PMid:24304645 PMCid:PMC4235049

66. Nagpal G, Usmani SS, Dhanda SK, Kaur H, Singh S, Sharma M, Raghava GP. Computer-aided designing of immunosuppressive peptides based on IL-10 inducing potential. Scientific reports. 2017 Feb 17;7:42851.
https://doi.org/10.1038/srep42851
PMid:28211521 PMCid:PMC5314457

67. Mehla, K. and Ramana, J., 2016. Identification of epitope-based peptide vaccine candidates against enterotoxigenic Escherichia coli: a comparative genomics and immunoinformatics approach. Molecular BioSystems, 12(3), pp.890-901.
https://doi.org/10.1039/C5MB00745C
PMid:26766131

68. Thomsen M, Lundegaard C, Buus S, Lund O, Nielsen M. MHCcluster, a method for functional clustering of MHC molecules. Immunogenetics. 2013 Sep;65(9):655-65.
https://doi.org/10.1007/s00251-013-0714-9
PMid:23775223 PMCid:PMC3750724

69. Ishimoto H, Mukae H, Date Y, Shimbara T, Mondal MS, Ashitani J, Hiratsuka T, Kubo S, Kohno S, Nakazato M. Identification of hBD-3 in respiratory tract and serum: the increase in pneumonia. European Respiratory Journal. 2006 Feb 1;27(2):253-60.
https://doi.org/10.1183/09031936.06.00105904
PMid:16452577

70. Judge CJ, Reyes-Aviles E, Conry SJ, Sieg SS, Feng Z, Weinberg A, Anthony DD. HBD-3 induces NK cell activation, IFN-γ secretion and mDC dependent cytolytic function. Cellular immunology. 2015 Oct 1;297(2):61-8.
https://doi.org/10.1016/j.cellimm.2015.06.004
PMid:26302933 PMCid:PMC4682877

71. Leikina E, Delanoe-Ayari H, Melikov K, Cho MS, Chen A, Waring AJ, Wang W, Xie Y, Loo JA, Lehrer RI, Chernomordik LV. Carbohydrate-binding molecules inhibit viral fusion and entry by crosslinking membrane glycoproteins. Nature immunology. 2005 Oct;6(10):995-1001.
https://doi.org/10.1038/ni1248
PMid:16155572

72. Arai, R., Ueda, H., Kitayama, A., Kamiya, N. and Nagamune, T., 2001. Design of the linkers which effectively separate domains of a bifunctional fusion protein. Protein engineering, 14(8), pp.529-532.
https://doi.org/10.1093/protein/14.8.529
PMid:11579220

73. Tahir Ul Qamar, M., Shokat, Z., Muneer, I., Ashfaq, U. A., Javed, H., Anwar, F., Bari, A., Zahid, B., & Saari, N. (2020). Multiepitope-Based Subunit Vaccine Design and Evaluation against Respiratory Syncytial Virus Using Reverse Vaccinology Approach. Vaccines, 8(2), 288.
https://doi.org/10.3390/vaccines8020288
PMid:32521680 PMCid:PMC7350008

74. Syeda Tahira Qousain Naqvi, Mamoona Yasmeen, Mehreen Ismail, Syed Aun Muhammad, Syed Nawazish-i-Husain, Amjad Ali, Fahad Munir, QiYu Zhang, "Designing of Potential Polyvalent Vaccine Model for Respiratory Syncytial Virus by System Level Immunoinformatics Approaches", BioMed Research International, vol. 2021, Article ID 9940010, 18 pages, 2021.
https://doi.org/10.1155/2021/9940010
PMid:34136576 PMCid:PMC8177976

75. Gu, Y., Sun, X., Li, B., Huang, J., Zhan, B. and Zhu, X., 2017. Vaccination with a paramyosin-based multi-epitope vaccine elicits significant protective immunity against Trichinella spiralis infection in mice. Frontiers in microbiology, 8, p.1475.
https://doi.org/10.3389/fmicb.2017.01475
PMid:28824599 PMCid:PMC5540943

76. Magnan, C.N., Randall, A. and Baldi, P., 2009. SOLpro: accurate sequence-based prediction of protein solubility. Bioinformatics, 25(17), pp.2200-2207.
https://doi.org/10.1093/bioinformatics/btp386
PMid:19549632

77. Saha S, Raghava GP. AlgPred: prediction of allergenic proteins and mapping of IgE epitopes. Nucleic acids research. 2006 Jul 1;34(suppl_2):W202-9.
https://doi.org/10.1093/nar/gkl343
PMid:16844994 PMCid:PMC1538830

78. Ullah A, Sarkar B, Islam SS. Exploiting the reverse vaccinology approach to design novel subunit vaccine against ebola virus. Immunobiology. 2020a May 1:151949.

https://doi.org/10.1101/2020.01.02.20016311

79. Hebditch, M., Carballo-Amador, M.A., Charonis, S., Curtis, R. and Warwicker, J., 2017. Protein-Sol: a web tool for predicting protein solubility from sequence. Bioinformatics, 33(19), pp.3098-3100.
https://doi.org/10.1093/bioinformatics/btx345
PMid:28575391 PMCid:PMC5870856

80. Buchan DW, Jones DT. The PSIPRED protein analysis workbench: 20 years on. Nucleic acids research. 2019 Jul 2;47(W1):W402-7.
https://doi.org/10.1093/nar/gkz297
PMid:31251384 PMCid:PMC6602445

81. Jones DT. Protein secondary structure prediction based on position-specific scoring matrices. Journal of molecular biology. 1999 Sep 17;292(2):195-202.
https://doi.org/10.1006/jmbi.1999.3091
PMid:10493868

82. Garnier J, Gibrat JF, Robson B. [32] GOR method for predicting protein secondary structure from amino acid sequence. InMethods in enzymology 1996 Jan 1 (Vol. 266, pp. 540-553). Academic Press.
https://doi.org/10.1016/S0076-6879(96)66034-0

83. Geourjon C, Deleage G. SOPMA: significant improvements in protein secondary structure prediction by consensus prediction from multiple alignments. Bioinformatics. 1995 Dec 1;11(6):681-4.
https://doi.org/10.1093/bioinformatics/11.6.681
PMid:8808585

84. Levin JM, Robson B, Garnier J. An algorithm for secondary structure determination in proteins based on sequence similarity. FEBS letters. 1986 Sep 15;205(2):303-8
https://doi.org/10.1016/0014-5793(86)80917-6

85. Källberg, M., Wang, H., Wang, S., Peng, J., Wang, Z., Lu, H., Xu, J., 2012. Template-based protein structure modeling using the RaptorX web server. Nat. protoc. 7, 1511.
https://doi.org/10.1038/nprot.2012.085
PMid:22814390 PMCid:PMC4730388

86. Wang S, Li W, Zhang R, Liu S, Xu J. CoinFold: a web server for protein contact prediction and contact-assisted protein folding. Nucleic acids research. 2016 Apr 25;44(W1):W361-6.
https://doi.org/10.1093/nar/gkw307
PMid:27112569 PMCid:PMC4987891

87. Nugent, T., Cozzetto, D. and Jones, D.T., 2014. Evaluation of predictions in the CASP10 model refinement category. Proteins: Structure, Function, and Bioinformatics, 82, pp.98-111. https://doi.org/10.1002/prot.24377 PMid:23900810 PMCid:PMC4282348

88. Ko, J., Park, H., Heo, L. and Seok, C., 2012. GalaxyWEB server for protein structure prediction and refinement. Nucleic acids research, 40(W1), pp.W294-W297. https://doi.org/10.1093/nar/gks493 PMid:22649060 PMCid:PMC3394311

89. Laskowski, R.A., MacArthur, M.W. and Thornton, J.M., 2006. PROCHECK: validation of protein-structure coordinates.

90. Morris, A.L., MacArthur, M.W., Hutchinson, E.G. and Thornton, J.M., 1992. Stereochemical quality of protein structure coordinates. Proteins: Structure, Function, and Bioinformatics, 12(4), pp.345-364. https://doi.org/10.1002/prot.340120407 PMid:1579569

91. Wiederstein, M. and Sippl, M.J., 2007. ProSA-web: interactive web service for the recognition of errors in three-dimensional structures of proteins. Nucleic acids research, 35(suppl_2), pp.W407-W410. https://doi.org/10.1093/nar/gkm290 PMid:17517781 PMCid:PMC1933241

92. Craig, D.B. and Dombkowski, A.A., 2013. Disulfide by Design 2.0: a web-based tool for disulfide engineering in proteins. BMC bioinformatics, 14(1), p.346. https://doi.org/10.1186/1471-2105-14-346 PMid:24289175 PMCid:PMC3898251

93. Dombkowski AA. Disulfide by Design™: a computational method for the rational design of disulfide bonds in proteins. Bioinformatics. 2003 Sep 22;19(14):1852-3. https://doi.org/10.1093/bioinformatics/btg231 PMid:14512360

94. Dombkowski AA, Crippen GM. Disulfide recognition in an optimized threading potential. Protein engineering. 2000 Oct 1;13(10):679-89. https://doi.org/10.1093/protein/13.10.679 PMid:11112506

95. Dombkowski AA, Sultana KZ, Craig DB. Protein disulfide engineering. FEBS letters. 2014 Jan 21;588(2):206-12. https://doi.org/10.1016/j.febslet.2013.11.024 PMid:24291258

96. Petersen, M.T.N., Jonson, P.H., Petersen, S.B., 1999. Amino acid neighbours and detailed conformational analysis of cysteines in proteins. Protein Eng. 12, 535-548.
https://doi.org/10.1093/protein/12.7.535
PMid:10436079

97. Cai CZ, Han LY, Ji ZL, Chen X, Chen YZ. SVM-Prot: web-based support vector machine software for functional classification of a protein from its primary sequence. Nucleic acids research. 2003 Jul 1;31(13):3692-7.
https://doi.org/10.1093/nar/gkg600
PMid:12824396 PMCid:PMC169006

98. Steentoft C, Vakhrushev SY, Joshi HJ, Kong Y, Vester-Christensen MB, Schjoldager KT, Lavrsen K, Dabelsteen S, Pedersen NB, Marcos-Silva L, Gupta R. Precision mapping of the human O-GalNAc glycoproteome through SimpleCell technology. The EMBO journal. 2013 May 15;32(10):1478-88.
https://doi.org/10.1038/emboj.2013.79
PMid:23584533 PMCid:PMC3655468

99. Stern, L.J., Calvo-Calle, J.M., 2009. HLA-DR: molecular insights and vaccine design. Curr. Pharm. Des. 15, 3249-3261.
https://doi.org/10.2174/138161209789105171
PMid:19860674 PMCid:PMC3615543

100. Pierce BG, Wiehe K, Hwang H, Kim BH, Vreven T, Weng Z. ZDOCK server: interactive docking prediction of protein-protein complexes and symmetric multimers. Bioinformatics. 2014 Jun 15;30(12):1771-3.
https://doi.org/10.1093/bioinformatics/btu097
PMid:24532726 PMCid:PMC4058926

101. Berendsen HJ, van der Spoel D, van Drunen R. GROMACS: a message-passing parallel molecular dynamics implementation. Computer physics communications. 1995 Sep 2;91(1-3):43-56.
https://doi.org/10.1016/0010-4655(95)00042-E

102. Best RB, Zhu X, Shim J, Lopes PE, Mittal J, Feig M, MacKerell Jr AD. Optimization of the additive CHARMM all-atom protein force field targeting improved sampling of the backbone ϕ, ψ and side-chain $\chi 1$ and $\chi 2$ dihedral angles. Journal of chemical theory and computation. 2012 Sep 11;8(9):3257-73.
https://doi.org/10.1021/ct300400x
PMid:23341755 PMCid:PMC3549273

103. Vanommeslaeghe K, Hatcher E, Acharya C, Kundu S, Zhong S, Shim J, Darian E, Guvench O, Lopes P, Vorobyov I, Mackerell Jr AD. CHARMM general force field: A force field for drug-like molecules compatible with the CHARMM all-atom additive biological force fields. Journal of computational chemistry. 2010 Mar;31(4):671-90.

https://doi.org/10.1002/jcc.21367
PMid:19575467 PMCid:PMC2888302

104. Zielkiewicz J. Structural properties of water: Comparison of the SPC, SPCE, TIP4P, and TIP5P models of water. The Journal of chemical physics. 2005 Sep 8;123(10):104501.
https://doi.org/10.1063/1.2018637
PMid:16178604

105. Bussi G, Donadio D, Parrinello M. Canonical sampling through velocity rescaling. The Journal of chemical physics. 2007 Jan 7;126(1):014101.
https://doi.org/10.1063/1.2408420
PMid:17212484

106. Berendsen HJ, Postma JV, van Gunsteren WF, DiNola AR, Haak JR. Molecular dynamics with coupling to an external bath. The Journal of chemical physics. 1984 Oct 15;81(8):3684-90.
https://doi.org/10.1063/1.448118

107. Parrinello M, Rahman A. Polymorphic transitions in single crystals: A new molecular dynamics method. Journal of Applied physics. 1981 Dec;52(12):7182-90.
https://doi.org/10.1063/1.328693

108. Hess B, Bekker H, Berendsen HJ, Fraaije JG. LINCS: a linear constraint solver for molecular simulations. Journal of computational chemistry. 1997 Sep;18(12):1463-72.
https://doi.org/10.1002/(SICI)1096-987X(199709)18:12<1463::AID-JCC4>3.0.CO;2-H

109. Petersen HG. Accuracy and efficiency of the particle mesh Ewald method. The Journal of chemical physics. 1995 Sep 1;103(9):3668-79.
https://doi.org/10.1063/1.470043

110. Rapin, N., Lund, O., Bernaschi, M. and Castiglione, F., 2010. Computational immunology meets bioinformatics: the use of prediction tools for molecular binding in the simulation of the immune system. PLoS One, 5(4).
https://doi.org/10.1371/journal.pone.0009862
PMid:20419125 PMCid:PMC2855701

111. Castiglione, F., Mantile, F., De Berardinis, P. and Prisco, A., 2012. How the interval between prime and boost injection affects the immune response in a computational model of the immune system. Computational and mathematical methods in medicine, 2012.
https://doi.org/10.1155/2012/842329
PMid:22997539 PMCid:PMC3446774

112. Sarkar B, Ullah MA, Araf Y, Das S, Rahman MH, Moin AT. Designing novel epitope-based polyvalent vaccines against herpes simplex virus-1 and 2 exploiting the immunoinformatics approach. Journal of Biomolecular Structure and Dynamics. 2020b Aug 6:1-21.
https://doi.org/10.1080/07391102.2020.1803969
PMid:32762514

113. Grote A, Hiller K, Scheer M, Münch R, Nörtemann B, Hempel DC, Jahn D. JCat: a novel tool to adapt codon usage of a target gene to its potential expression host. Nucleic Acids Res 2005;33:W526-31.
https://doi.org/10.1093/nar/gki376
PMid:15980527 PMCid:PMC1160137

114. Chang KY, Yang JR. Analysis and prediction of highly effective antiviral peptides based on random forests. PloS one. 2013 Aug 5;8(8):e70166.
https://doi.org/10.1371/journal.pone.0070166
PMid:23940542 PMCid:PMC3734225

115. Choi ES, Lee SG, Lee SJ, Kim E. Rapid detection of 6×-histidine-labeled recombinant proteins by immunochromatography using dye-labeled cellulose nanobeads. Biotechnology letters. 2015 Mar;37(3):627-32.
https://doi.org/10.1007/s10529-014-1731-y
PMid:25388454

116. Solanki, V. and Tiwari, V., 2018. Subtractive proteomics to identify novel drug targets and reverse vaccinology for the development of chimeric vaccine against Acinetobacter baumannii. Scientific reports, 8(1), pp.1-19.
https://doi.org/10.1038/s41598-018-26689-7
PMid:29899345 PMCid:PMC5997985

117. Biswal, J.K., Bisht, P., Mohapatra, J.K., Ranjan, R., Sanyal, A. and Pattnaik, B., 2015. Application of a recombinant capsid polyprotein (P1) expressed in a prokaryotic system to detect antibodies against foot-and-mouth disease virus serotype O. Journal of virological methods, 215, pp.45-51.
https://doi.org/10.1016/j.jviromet.2015.02.008
PMid:25701759

118. Zuker, M., 2003. Mfold web server for nucleic acid folding and hybridization prediction. Nucleic acids research, 31(13), pp.3406-3415.
https://doi.org/10.1093/nar/gkg595
PMid:12824337 PMCid:PMC169194

119. Mathews, D.H., Sabina, J., Zuker, M. and Turner, D.H., 1999. Expanded sequence dependence of thermodynamic parameters improves prediction of RNA secondary structure. Journal of molecular biology, 288(5), pp.911-940.
https://doi.org/10.1006/jmbi.1999.2700

PMid:10329189

120. Mathews, D.H., Turner, D.H. and Zuker, M., 2007. RNA secondary structure prediction. Current protocols in nucleic acid chemistry, 28(1), pp.11-2.
https://doi.org/10.1002/0471142700.nc1102s28
PMid:18428968 PMCid:PMC5115178

121. Khan MT, Islam R, Jerin TJ, Mahmud A, Khatun S, Kobir A, Islam MN, Akter A, Mondal SI. Immunoinformatics and molecular dynamics approaches: Next generation vaccine design against West Nile virus. Plos one. 2021 Jun 17;16(6):e0253393.
https://doi.org/10.1371/journal.pone.0253393
PMid:34138958 PMCid:PMC8211291

122. Lobanov MYu, Bogatyreva NS, Galzitskaya OV. Radius of gyration as an indicator of protein structure compactness. Mol Biol. 2008 Aug;42(4):623-8.
https://doi.org/10.1134/S0026893308040195

123. Pettersen EF, Goddard TD, Huang CC, Meng EC, Couch GS, Croll TI, et al. UCSF ChimeraX : Structure visualization for researchers, educators, and developers. Protein Science. 2021 Jan;30(1):70-82.
https://doi.org/10.1002/pro.3943
PMid:32881101 PMCid:PMC7737788

124. Ndure J, Flanagan KL. Targeting regulatory T cells to improve vaccine immunogenicity in early life. Frontiers in microbiology. 2014 Sep 11;5:477.
https://doi.org/10.3389/fmicb.2014.00477
PMid:25309517 PMCid:PMC4161046

125. Carbone A, Zinovyev A, Képes F. Codon adaptation index as a measure of dominating codon bias. Bioinformatics 2003;19:2005-15.
https://doi.org/10.1093/bioinformatics/btg272
PMid:14594704

126. Gallagher TM, Buchmeier MJ. Coronavirus spike proteins in viral entry and pathogenesis. Virology. 2001;279(2):pp.371-374.
https://doi.org/10.1006/viro.2000.0757
PMid:11162792 PMCid:PMC7133764

127. Almofti YA, Abd-elrahman KA, Gassmallah SAE, et al. Multi epitopes vaccine prediction against severe acute respiratory syndrome (sars) coronavirus using immunoinformatics approaches. Am J Microbiol Res. 2018;6(3):pp.94-114.
https://doi.org/10.12691/ajmr-6-3-5

128. Carvalho LH, Sano GI, Hafalla JC, et al. IL-4-secreting CD4+ T cells are crucial to the development of CD8+ T-cell responses against malaria liver stages. Nat Med. 2002;8(2):pp.166-170.
https://doi.org/10.1038/nm0202-166
PMid:11821901

129. Shey RA, Ghogomu SM, Esoh KK, et al. In-silico design of a multi-epitope vaccine candidate against onchocerciasis and related filarial diseases. Sci Rep. 2019;9(1):pp.1-18.
https://doi.org/10.1038/s41598-019-40833-x
PMid:30867498 PMCid:PMC6416346

130. Hoque MN, Istiaq A, Clement RA, et al. Metagenomic deep sequencing reveals association of microbiome signature with functional biases in bovine mastitis. Sci Rep. 2019;9(1):pp.1-14.
https://doi.org/10.1038/s41598-019-49468-4
PMid:31537825 PMCid:PMC6753130

131. Kambayashi T, Laufer TM. Atypical MHC class II-expressing antigen-presenting cells: can anything replace a dendritic cell? Nat Rev Immunol. 2014;14(11):pp.719-730.
https://doi.org/10.1038/nri3754
PMid:25324123

132. Štěpánová S, Kašička V. Application of Capillary Electromigration Methods for Physicochemical Measurements. InCapillary Electromigration Separation Methods 2018 Jan 1 (pp. 547-591). Elsevier.
https://doi.org/10.1016/B978-0-12-809375-7.00024-1

133. Hamasaki-Katagiri N, Lin BC, Simon J, Hunt RC, Schiller T, Russek-Cohen E, Komar AA, Bar H, Kimchi-Sarfaty C. The importance of mRNA structure in determining the pathogenicity of synonymous and non-synonymous mutations in haemophilia. Haemophilia. 2017 Jan;23(1):e8-17.
https://doi.org/10.1111/hae.13107
PMid:27933712 PMCid:PMC5226872

134. Ikai, A., 1980. Thermostability and aliphatic index of globular proteins. The Journal of Biochemistry, 88(6), pp.1895-1898.

135. Panda, S. and Chandra, G., 2012. Physicochemical characterization and functional analysis of some snake venom toxin proteins and related non-toxin proteins of other chordates. Bioinformation, 8(18), p.891.
https://doi.org/10.6026/97320630008891
PMid:23144546 PMCid:PMC3489095

136. Pei H, Liu J, Cheng Y, Sun C, Wang C, Lu Y, Ding J, Zhou J, Xiang H. Expression of SARS-coronavirus nucleocapsid protein in Escherichia coli and Lactococcus lactis for

serodiagnosis and mucosal vaccination. Applied microbiology and biotechnology. 2005 Aug;68(2):220-7.
https://doi.org/10.1007/s00253-004-1869-y
PMid:15660214 PMCid:PMC7079895

137. Morla S, Makhija A, Kumar S. Synonymous codon usage pattern in glycoprotein gene of rabies virus. Gene. 2016 Jun 10;584(1):1-6.
https://doi.org/10.1016/j.gene.2016.02.047
PMid:26945626

138. Kyte J, Doolittle RF. A simple method for displaying the hydropathic character of a protein. Journal of molecular biology. 1982 May 5;157(1):105-32.
https://doi.org/10.1016/0022-2836(82)90515-0

139. Chang, K.Y. and Yang, J.R., 2013. Analysis and prediction of highly effective antiviral peptides based on random forests. PloS one, 8(8).
https://doi.org/10.1371/journal.pone.0070166
PMid:23940542 PMCid:PMC3734225

140. Zhang, L. (2018). Multi-epitope vaccines: A promising strategy against tumors and viral infections. Cellular & Molecular Immunology, 15(2), 182-184.
https://doi.org/10.1038/cmi.2017.92
PMid:28890542 PMCid:PMC5811687

141. Bacchetta, R., Gregori, S., & Roncarolo, M. G. (2005). CD4þ regulatory T cells: Mechanisms of induction and effector function. Autoimmunity Reviews, 4(8), 491-496.
https://doi.org/10.1016/j.autrev.2005.04.005
PMid:16214084

142. Cano, R.L.E. and Lopera, H.D.E., 2013. Introduction to T and B lymphocytes. In Autoimmunity: From Bench to Bedside [Internet]. El Rosario University Press.

143. Raza MT, Mizan S, Yasmin F, Akash AS, Shahik SM. Epitope-based universal vaccine for Human T-lymphotropic virus-1 (HTLV-1). PloS one. 2021 Apr 2;16(4):e0248001.
https://doi.org/10.1371/journal.pone.0248001
PMid:33798232 PMCid:PMC8018625

144. Sanchez-Trincado JL, Gomez-Perosanz M, Reche PA. Fundamentals and methods for T- and B-cell epitope prediction. Journal of immunology research. 2017 Oct;2017.
https://doi.org/10.1155/2017/2680160
PMid:29445754 PMCid:PMC5763123

145. Shachar I, Karin N. The dual roles of inflammatory cytokines and chemokines in the regulation of autoimmune diseases and their clinical implications. Journal of leukocyte biology. 2013 Jan;93(1):51-61.

https://doi.org/10.1189/jlb.0612293
PMid:22949334

146. Holdsworth SR, Gan PY. Cytokines: names and numbers you should care about. Clinical journal of the American Society of Nephrology. 2015 Dec 7;10(12):2243-54.
https://doi.org/10.2215/CJN.07590714
PMid:25941193 PMCid:PMC4670773

147. Cavaillon JM. Pro-versus anti-inflammatory cytokines: myth or reality. CELLULAR AND MOLECULAR BIOLOGY-PARIS-WEGMANN-. 2001 Jun 1;47(4):695-702.

148. Turner MD, Nedjai B, Hurst T, Pennington DJ. Cytokines and chemokines: At the crossroads of cell signalling and inflammatory disease. Biochimica et Biophysica Acta (BBA)-Molecular Cell Research. 2014 Nov 1;1843(11):2563-82.
https://doi.org/10.1016/j.bbamcr.2014.05.014
PMid:24892271

149. CHANG HD, Radbruch A. The pro-and anti-inflammatory potential of interleukin-12. Annals of the New York Academy of Sciences. 2007 Aug;1109(1):40-6.
https://doi.org/10.1196/annals.1398.006
PMid:17785289

150. van Schaik SM, Obot N, Enhorning G, Hintz K, Gross K, Hancock GE, Stack AM, Welliver RC. Role of interferon gamma in the pathogenesis of primary respiratory syncytial virus infection in BALB/c mice. Journal of medical virology. 2000 Oct;62(2):257-66.
https://doi.org/10.1002/1096-9071(200010)62:2<257::AID-JMV19>3.0.CO;2-M

151. Sarkar SN, Sen GC. Novel functions of proteins encoded by viral stress-inducible genes. Pharmacology & therapeutics. 2004 Sep 1;103(3):245-59.
https://doi.org/10.1016/j.pharmthera.2004.07.007
PMid:15464592

152. Fuse S, Molloy MJ, Usherwood EJ. Immune responses against persistent viral infections: possible avenues for immunotherapeutic interventions. Critical Reviews™ in Immunology. 2008;28(2).
https://doi.org/10.1615/CritRevImmunol.v28.i2.40
PMid:18540829

153. Junttila IS. Tuning the cytokine responses: an update on interleukin (IL)-4 and IL-13 receptor complexes. Frontiers in immunology. 2018 Jun 7;9:888.
https://doi.org/10.3389/fimmu.2018.00888
PMid:29930549 PMCid:PMC6001902

154. Abinaya RV, Viswanathan P. Biotechnology-based therapeutics. InTranslational Biotechnology 2021 Jan 1 (pp. 27-52). Academic Press.

https://doi.org/10.1016/B978-0-12-821972-0.00019-8
PMid:32660413

155. Funderburg N, Lederman MM, Feng Z, Drage MG, Jadlowsky J, Harding CV, Weinberg A, Sieg SF. Human β-defensin-3 activates professional antigen-presenting cells via Toll-like receptors 1 and 2. Proceedings of the National Academy of Sciences. 2007 Nov 20;104(47):18631-5.
https://doi.org/10.1073/pnas.0702130104
PMid:18006661 PMCid:PMC2141828

156. Judge CJ, Reyes-Aviles E, Conry SJ, Sieg SS, Feng Z, Weinberg A, Anthony DD. HBD-3 induces NK cell activation, IFN-γ secretion and mDC dependent cytolytic function. Cellular immunology. 2015 Oct 1;297(2):61-8.
https://doi.org/10.1016/j.cellimm.2015.06.004
PMid:26302933 PMCid:PMC4682877

157. Funderburg N, Lederman MM, Feng Z, Drage MG, Jadlowsky J, Harding CV, Weinberg A, Sieg SF. Human β-defensin-3 activates professional antigen-presenting cells via Toll-like receptors 1 and 2. Proceedings of the National Academy of Sciences. 2007 Nov 20;104(47):18631-5.
https://doi.org/10.1073/pnas.0702130104
PMid:18006661 PMCid:PMC2141828

158. Wolk K, Kunz S, Witte E, Friedrich M, Asadullah K, Sabat R. IL-22 increases the innate immunity of tissues. Immunity. 2004 Aug 1;21(2):241-54.
https://doi.org/10.1016/j.immuni.2004.07.007
PMid:15308104

159. Sørensen OE, Cowland JB, Theilgaard-Mönch K, Liu L, Ganz T, Borregaard N. Wound healing and expression of antimicrobial peptides/polypeptides in human keratinocytes, a consequence of common growth factors. The Journal of Immunology. 2003 Jun 1;170(11):5583-9.
https://doi.org/10.4049/jimmunol.170.11.5583
PMid:12759437

160. Ferris LK, Mburu YK, Mathers AR, Fluharty ER, Larregina AT, Ferris RL, Falo Jr LD. Human beta-defensin 3 induces maturation of human Langerhans cell-like dendritic cells: an antimicrobial peptide that functions as an endogenous adjuvant. Journal of Investigative Dermatology. 2013 Feb 1;133(2):460-8.
https://doi.org/10.1038/jid.2012.319
PMid:22951718 PMCid:PMC3521079

161. Joly S, Organ CC, Johnson GK, McCray Jr PB, Guthmiller JM. Correlation between β-defensin expression and induction profiles in gingival keratinocytes. Molecular immunology. 2005 May 1;42(9):1073-84.
https://doi.org/10.1016/j.molimm.2004.11.001

PMid:15829297

162. Judge CJ, Reyes-Aviles E, Conry SJ, Sieg SS, Feng Z, Weinberg A, Anthony DD. HBD-3 induces NK cell activation, IFN-γ secretion and mDC dependent cytolytic function. Cellular immunology. 2015 Oct 1;297(2):61-8.
https://doi.org/10.1016/j.cellimm.2015.06.004
PMid:26302933 PMCid:PMC4682877

163. Röhrl J, Yang D, Oppenheim JJ, Hehlgans T. Human β-defensin 2 and 3 and their mouse orthologs induce chemotaxis through interaction with CCR2. The Journal of Immunology. 2010 Jun 15;184(12):6688-94.
https://doi.org/10.4049/jimmunol.0903984
PMid:20483750 PMCid:PMC6309988

164. Shental-Bechor D, Levy Y. Effect of glycosylation on protein folding: a close look at thermodynamic stabilization. Proceedings of the National Academy of Sciences. 2008 Jun 17;105(24):8256-61.
https://doi.org/10.1073/pnas.0801340105
PMid:18550810 PMCid:PMC2448824

165. Ojha R, Prajapati VK. Cognizance of posttranslational modifications in vaccines: A way to enhanced immunogenicity. Journal of Cellular Physiology. 2021 Jun 25.
https://doi.org/10.1002/jcp.30483
PMid:34170014 PMCid:PMC8427110

166. Zarling AL, Ficarro SB, White FM, Shabanowitz J, Hunt DF, Engelhard VH. Phosphorylated peptides are naturally processed and presented by major histocompatibility complex class I molecules in vivo. The Journal of experimental medicine. 2000 Dec 18;192(12):1755-62.
https://doi.org/10.1084/jem.192.12.1755
PMid:11120772 PMCid:PMC2213507

167. Kawai T, Akira S. TLR signaling. InSeminars in immunology 2007 Feb 1 (Vol. 19, No. 1, pp. 24-32). Academic Press.
https://doi.org/10.1016/j.smim.2006.12.004
PMid:17275323

168. Murawski MR, Bowen GN, Cerny AM, Anderson LJ, Haynes LM, Tripp RA, Kurt-Jones EA, Finberg RW. Respiratory syncytial virus activates innate immunity through Toll-like receptor 2. Journal of virology. 2009 Feb 1;83(3):1492-500.
https://doi.org/10.1128/JVI.00671-08
PMid:19019963 PMCid:PMC2620898

169. Akira S, Uematsu S, Takeuchi O. Pathogen recognition and innate immunity. Cell. 2006 Feb 24;124(4):783-801.
https://doi.org/10.1016/j.cell.2006.02.015

PMid:16497588

170. Cyr SL, Jones T, Stoica-Popescu I, Burt D, Ward BJ. C57Bl/6 mice are protected from respiratory syncytial virus (RSV) challenge and IL-5 associated pulmonary eosinophilic infiltrates following intranasal immunization with Protollin-eRSV vaccine. Vaccine. 2007 Apr 20;25(16):3228-32.
https://doi.org/10.1016/j.vaccine.2007.01.037
PMid:17374422

171. Hancock GE, Heers KM, Pryharski KS, Smith JD, Tiberio L. Adjuvants recognized by toll-like receptors inhibit the induction of polarized type 2 T cell responses by natural attachment (G) protein of respiratory syncytial virus. Vaccine. 2003 Oct 1;21(27-30):4348-58.
https://doi.org/10.1016/S0264-410X(03)00482-1

172. Janssen R, Pennings J, Hodemaekers H, Buisman A, van Oosten M, de Rond L, Öztürk K, Dormans J, Kimman T, Hoebee B. Host transcription profiles upon primary respiratory syncytial virus infection. Journal of virology. 2007 Jun 1;81(11):5958-67.
https://doi.org/10.1128/JVI.02220-06
PMid:17376894 PMCid:PMC1900269

173. Chang S, Dolganiuc A, Szabo G. Toll-like receptors 1 and 6 are involved in TLR2-mediated macrophage activation by hepatitis C virus core and NS3 proteins. Journal of leukocyte biology. 2007 Sep;82(3):479-87.
https://doi.org/10.1189/jlb.0207128
PMid:17595379

174. Compton T, Kurt-Jones EA, Boehme KW, Belko J, Latz E, Golenbock DT, Finberg RW. Human cytomegalovirus activates inflammatory cytokine responses via CD14 and Toll-like receptor 2. Journal of virology. 2003 Apr 15;77(8):4588-96.
https://doi.org/10.1128/JVI.77.8.4588-4596.2003
PMid:12663765 PMCid:PMC152130

175. Kurt-Jones EA, Chan M, Zhou S, Wang J, Reed G, Bronson R, Arnold MM, Knipe DM, Finberg RW. Herpes simplex virus 1 interaction with Toll-like receptor 2 contributes to lethal encephalitis. Proceedings of the National Academy of Sciences. 2004 Feb 3;101(5):1315-20.
https://doi.org/10.1073/pnas.0308057100
PMid:14739339 PMCid:PMC337050

176. Zhou S, Kurt-Jones EA, Mandell L, Cerny A, Chan M, Golenbock DT, Finberg RW. MyD88 is critical for the development of innate and adaptive immunity during acute lymphocytic choriomeningitis virus infection. European journal of immunology. 2005 Mar;35(3):822-30.
https://doi.org/10.1002/eji.200425730
PMid:15724245

177. Jin B, Sun T, Yu XH, Yang YX, Yeo AE. The effects of TLR activation on T-cell development and differentiation. Clinical and Developmental Immunology. 2012;2012. https://doi.org/10.1155/2012/836485 PMid:22737174 PMCid:PMC3376488

178. Gaddis DE, Michalek SM, Katz J. TLR4 signaling via MyD88 and TRIF differentially shape the CD4+ T cell response to Porphyromonas gingivalis hemagglutinin B. The Journal of Immunology. 2011 May 15;186(10):5772-83. https://doi.org/10.4049/jimmunol.1003192 PMid:21498664 PMCid:PMC3809913

179. Kaisho T, Hoshino K, Iwabe T, Takeuchi O, Yasui T, Akira S. Endotoxin can induce MyD88-deficient dendritic cells to support Th2 cell differentiation. International immunology. 2002 Jul 1;14(7):695-700. https://doi.org/10.1093/intimm/dxf039 PMid:12096028

180. Kurt-Jones EA, Popova L, Kwinn L, Haynes LM, Jones LP, Tripp RA, Walsh EE, Freeman MW, Golenbock DT, Anderson LJ, Finberg RW. Pattern recognition receptors TLR4 and CD14 mediate response to respiratory syncytial virus. Nature immunology. 2000 Nov;1(5):398-401. https://doi.org/10.1038/80833 PMid:11062499

181. Tayyari F, Marchant D, Moraes TJ, Duan W, Mastrangelo P, Hegele RG. Identification of nucleolin as a cellular receptor for human respiratory syncytial virus. Nature medicine. 2011 Sep;17(9):1132-5. https://doi.org/10.1038/nm.2444 PMid:21841784

182. Johnson TR, Rao S, Seder RA, Chen M, Graham BS. TLR9 agonist, but not TLR7/8, functions as an adjuvant to diminish FI-RSV vaccine-enhanced disease, while either agonist used as therapy during primary RSV infection increases disease severity. Vaccine. 2009 May 18;27(23):3045-52. https://doi.org/10.1016/j.vaccine.2009.03.026 PMid:19428918 PMCid:PMC2680782

183. Grassin-Delyle S, Abrial C, Salvator H, Brollo M, Naline E, Devillier P. The role of toll-like receptors in the production of cytokines by human lung macrophages. Journal of innate immunity. 2020;12(1):63-73. https://doi.org/10.1159/000494463 PMid:30557876 PMCid:PMC6959095

184. Almofti, Y.A., Abd-elrahman, K.A., Gassmallah, S.A.E. and Salih, M.A., 2018. Multi Epitopes Vaccine Prediction against Severe Acute Respiratory Syndrome (SARS) Coronavirus

Using Immunoinformatics Approaches. American Journal of Microbiological Research, 6(3), pp.94-114.
https://doi.org/10.12691/ajmr-6-3-5

185. Carvalho, L.H., Sano, G.I., Hafalla, J.C., Morrot, A., De Lafaille, M.A.C. and Zavala, F., 2002. IL-4-secreting CD4+ T cells are crucial to the development of CD8+ T-cell responses against malaria liver stages. Nature medicine, 8(2), pp.166-170.
https://doi.org/10.1038/nm0202-166
PMid:11821901

186. Shey, R.A., Ghogomu, S.M., Esoh, K.K., Nebangwa, N.D., Shintouo, C.M., Nongley, N.F., Asa, B.F., Ngale, F.N., Vanhamme, L. and Souopgui, J., 2019. In-silico design of a multi-epitope vaccine candidate against onchocerciasis and related filarial diseases. Scientific reports, 9(1), pp.1-18.
https://doi.org/10.1038/s41598-019-40833-x
PMid:30867498 PMCid:PMC6416346

187. Hoque, M.N., Istiaq, A., Clement, R.A., Sultana, M., Crandall, K.A., Siddiki, A.Z. and Hossain, M.A., 2019. Metagenomic deep sequencing reveals association of microbiome signature with functional biases in bovine mastitis. Scientific reports, 9(1), pp.1-14.
https://doi.org/10.1038/s41598-019-49468-4
PMid:31537825 PMCid:PMC6753130

188. Kambayashi, T. and Laufer, T.M., 2014. Atypical MHC class II-expressing antigen-presenting cells: can anything replace a dendritic cell?. Nature Reviews Immunology, 14(11), pp.719-730.
https://doi.org/10.1038/nri3754
PMid:25324123

189. Sarkar B, Ullah MA, Johora FT, Taniya MA, Araf Y. Immunoinformatics-guided designing of epitope-based subunit vaccine against the SARS Coronavirus-2 (SARS-CoV-2). Immunobiology. 2020c.
https://doi.org/10.1016/j.imbio.2020.151955
PMid:32517882 PMCid:PMC7211625

190. Russell MW, Moldoveanu Z, Ogra PL, Mestecky J. Mucosal immunity in COVID-19: a neglected but critical aspect of SARS-CoV-2 infection. Frontiers in Immunology. 2020 Nov 30;11:3221.
https://doi.org/10.3389/fimmu.2020.611337
PMid:33329607 PMCid:PMC7733922

191. Wilczyński J, Lukasik B, Torbicka E, Tranda I, Brzozowska-Binda A. Respiratory syncytial virus (RSV) antibodies in different immunoglobulin classes in small children. Acta Microbiologica Polonica. 1994 Jan 1;43(3-4):359-68.

192. Ndure J, Flanagan KL. Targeting regulatory T cells to improve vaccine immunogenicity in early life. Frontiers in microbiology. 2014 Sep 11;5:477.
https://doi.org/10.3389/fmicb.2014.00477
PMid:25309517 PMCid:PMC4161046

193. Sarkar B, Ullah MA, Araf Y. A systematic and reverse vaccinology approach to design novel subunit vaccines against dengue virus type-1 and human Papillomavirus-16. Informatics in Medicine Unlocked. 2020d May 16:100343.
https://doi.org/10.1016/j.imu.2020.100343

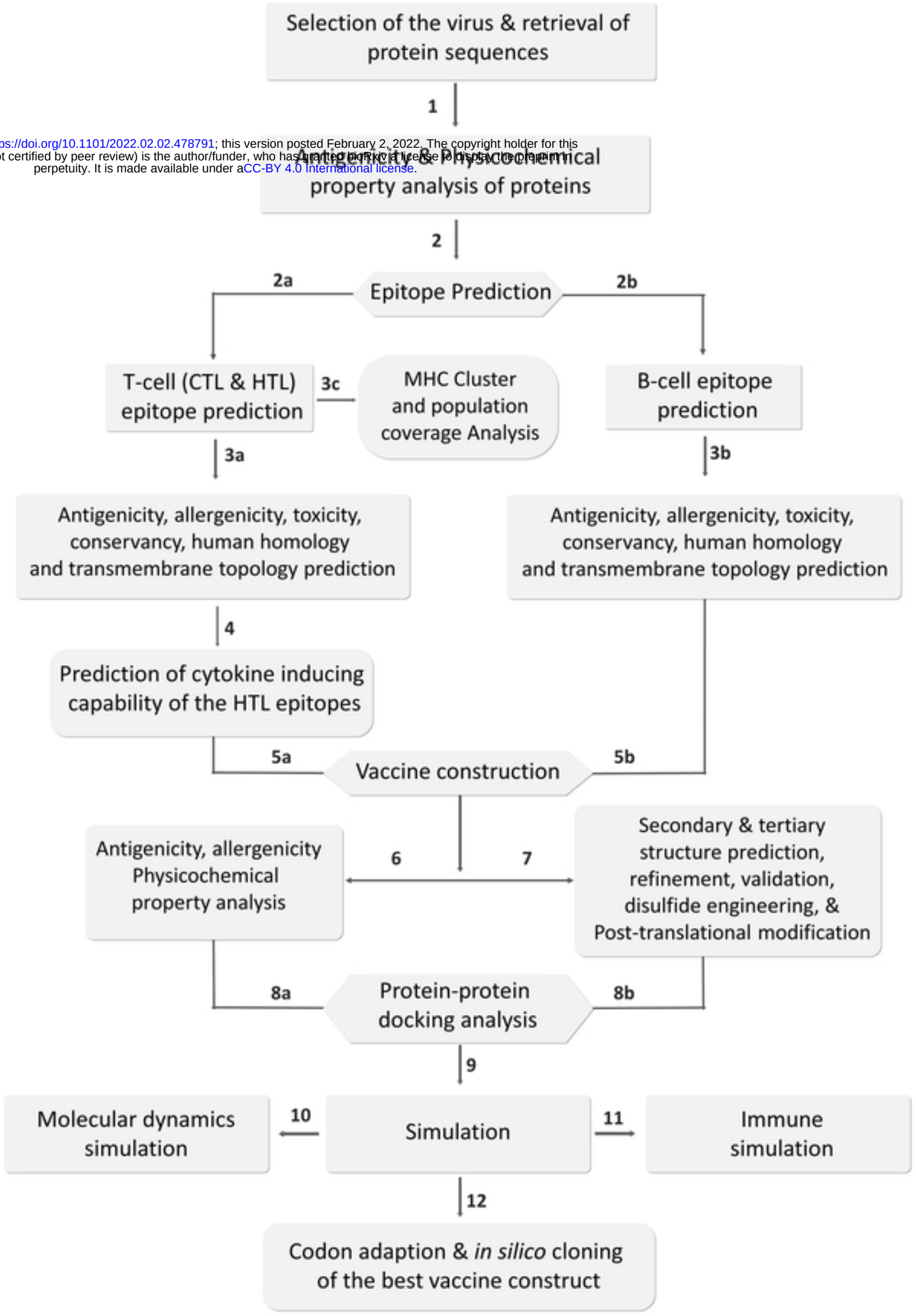

Fig 1

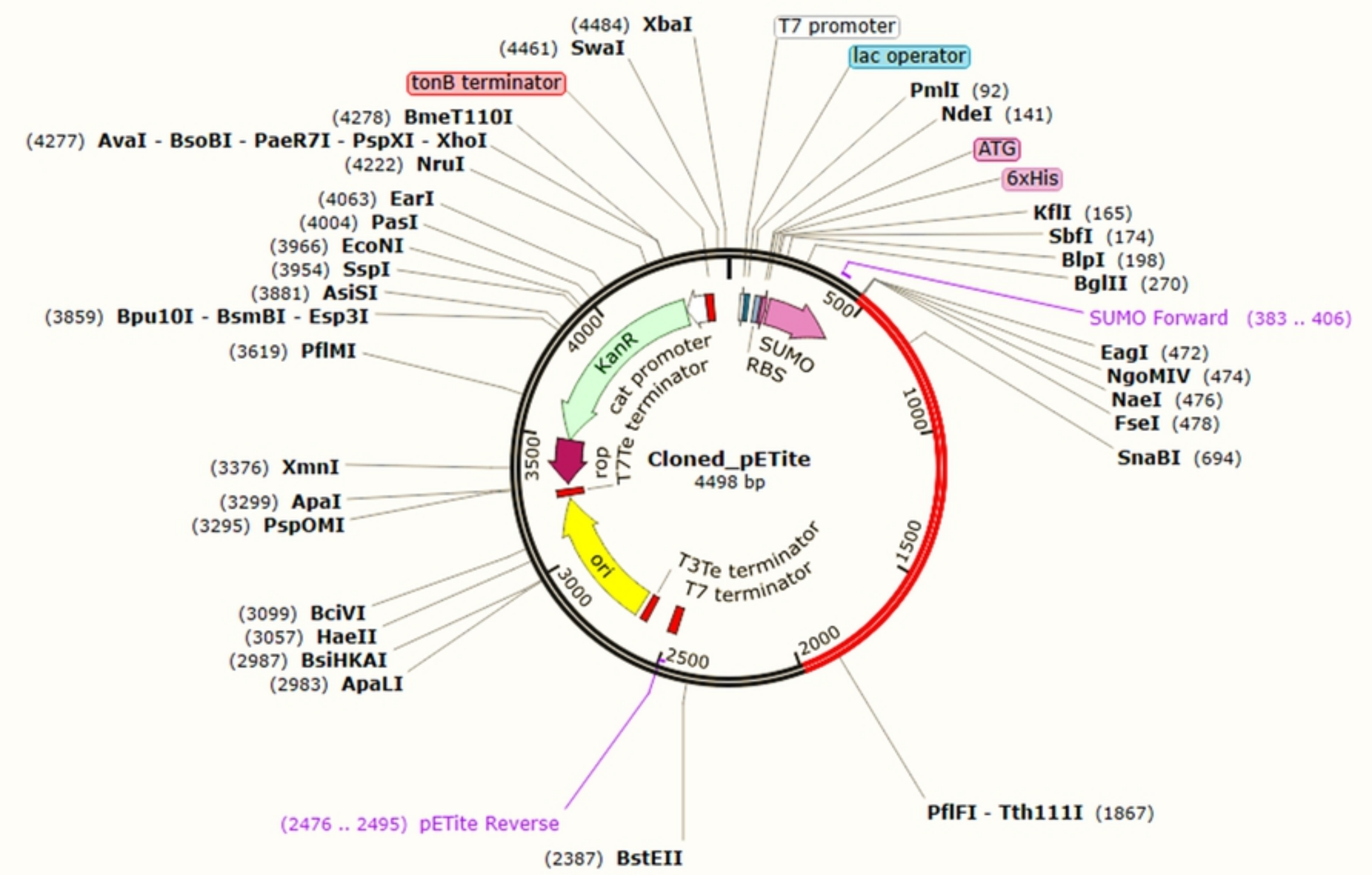
(4484) XbaI
(4461) SwaI
tonB terminator
(4278) BmeT110I
(4277) AvaI - BsoBI - PaeR7I - PspXI - XhoI
(4222) NruI
(4063) EarI
(4004) PasI
(3966) EcoNI
(3954) SspI
(3881) AsiSI
(3859) Bpu10I - BsmBI - Esp3I
(3619) PflMI
(3376) XmnI
(3299) ApaI
(3295) PspOMI
(3099) BciVI
(3057) HaeII
(2987) BsiHKAI
(2983) ApaLI
(2476 .. 2495) pETite Reverse
(2387) BstEII
T7 promoter
lac operator
PmlI (92)
NdeI (141)
ATG
6xHis
KflI (165)
SbfI (174)
BlpI (198)
BglII (270)
SUMO Forward (383 .. 406)
EagI (472)
NgoMIV (474)
NaeI (476)
FseI (478)
SnaBI (694)
PflFI - Tth111I (1867)
KanR
cat promoter
T7Te terminator
SUMO RBS
rop
T7Te terminator
ori
T3Te terminator
T7 terminator
Cloned_pETite
4498 bp
500
1000
1500
2000
2500
3000
3500
4000

Fig 10

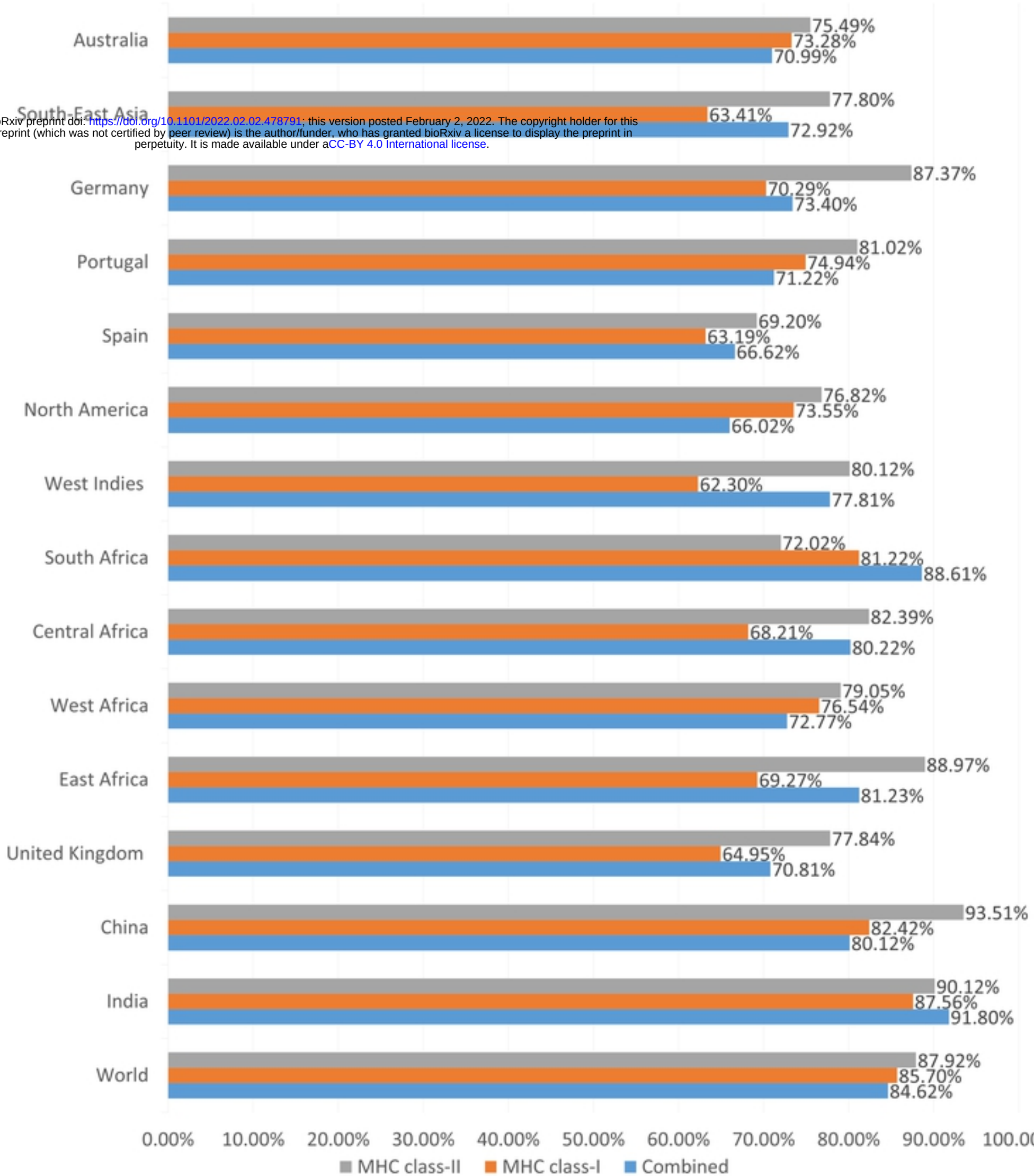

Fig 2

A

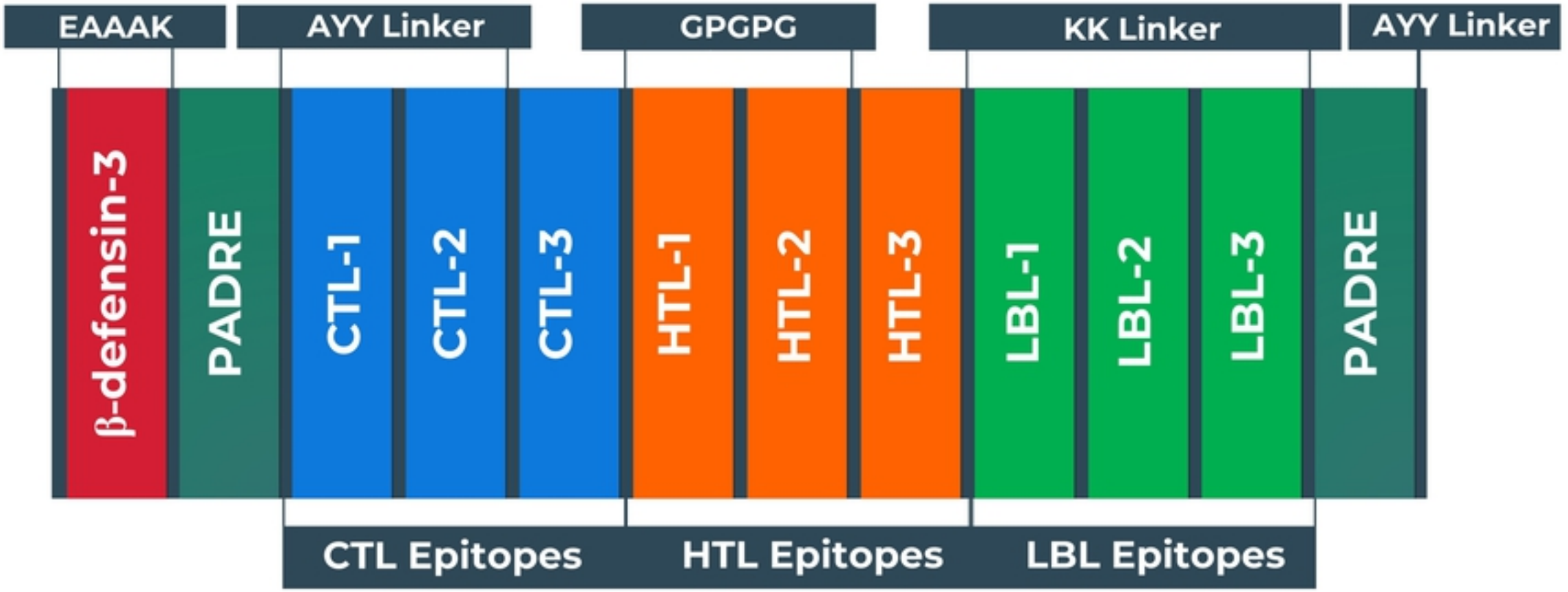

B

EAAAKGIINTLQKYYCRVRGGRCAVLSCLPKEEQIGKCSTRGRKCCRRKK**EAAA**
KAKFVAAWTLKAAA**AAY**VSLNPTSEK**AAY**QTNDNITAR**AAY**CIAALVITK**AAY**
RSGLTAVIR**AAY**SVKNIMLGH**AAY**KTNVTLSKK**AAY**KSALLSTNK**AAY**IASGV
AVSK**AAY**KQLLPIVNK**AAY**ITIELSNIK**AAY**LTSKVLDLK**AAY**TTTQTQPSK**AAY**
IFIASANHK**GPGPG**LGMLHTLVVASAGPT**GPGPG**LHTLVVASAGPTSAR**GPGP**
GEVLTLASLTTEIQIN**GPGPG**IVIIVILLSLIAVGL**GPGPG**VIIVILLSLIAVGLL**GP**
GPGEEFYQSTCSAVSKGY**GPGPG**LSILAMIISTSLIIA**GPGPG**TLSILAMIISTSLII
GPGPGQNPQLGISPSNPSEI**KK**PEFHGEDANNR**KK**EVTKESPITSNSTIINPTNET
DDTAGNKPNYQRK**KK**SFKEDPTPSDNPFS**KK**RNEESEKMAKDTSDEVSLNPTSE
K**KK**EVAPEYRHDSPD**KK**EYRGTPRNQDLYDA**KK**VFPSDEFDASISQVNEK**KK**T
SQIKNTTPTYLTQNPQLGISPSNPSEITS**KK**IPNKKPGKKTTTKPTKKPTLKTTKKD
PKPQTTKSKEVPTTKPTEEPTINTT**KK**SNTTGNPELTSQ**KK**AKFVAAWTLKAAA
AAY

Fig 3

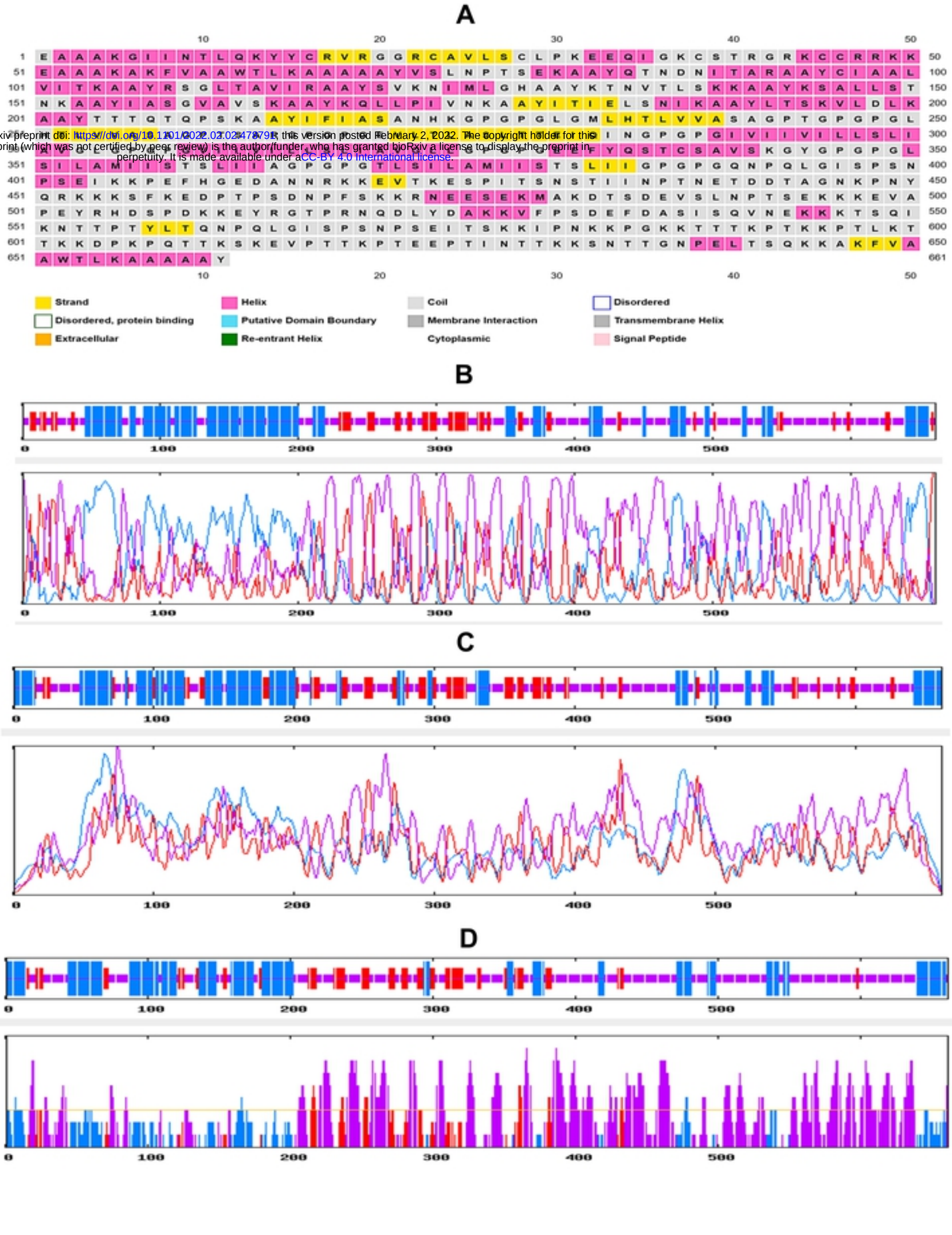

Fig 4

A

B

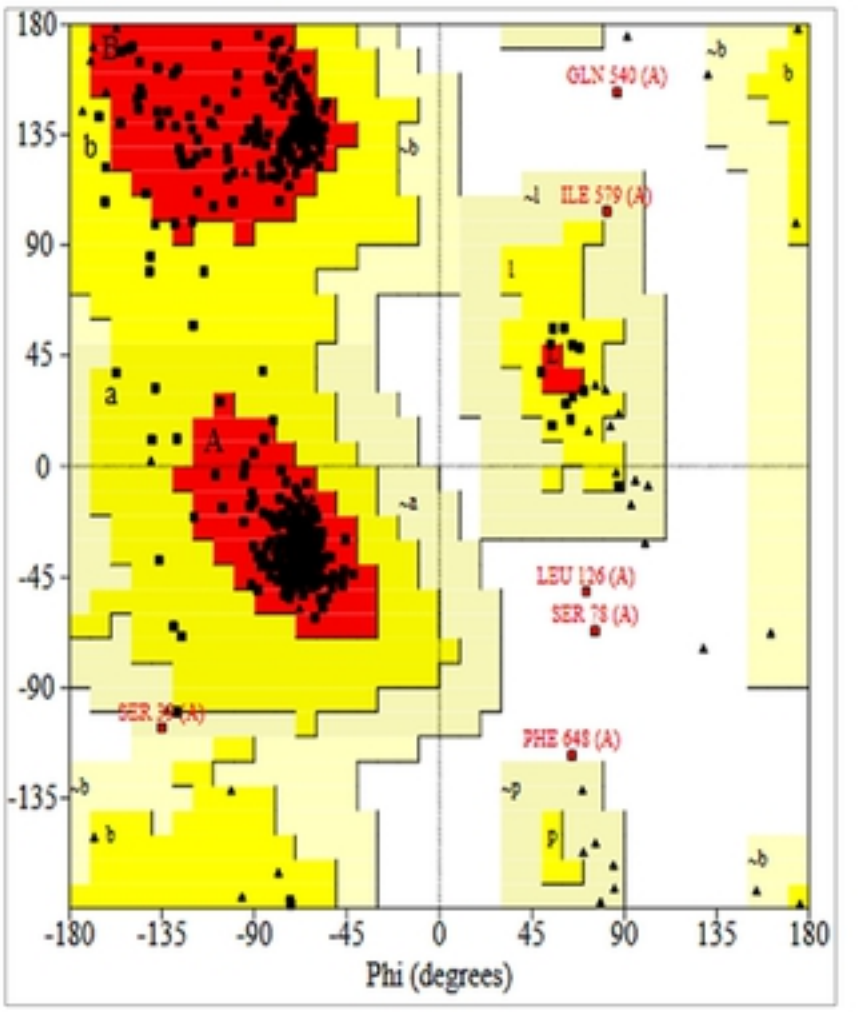

C

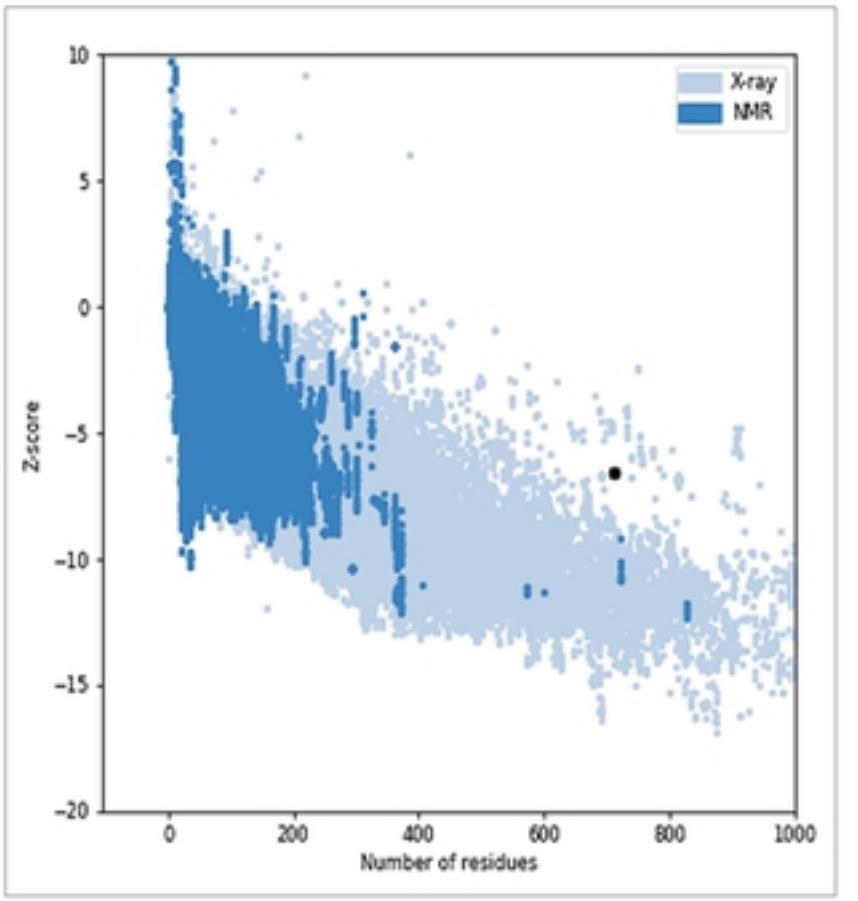

Fig 5

https://doi.org/10.1101/2022.02.02.478791

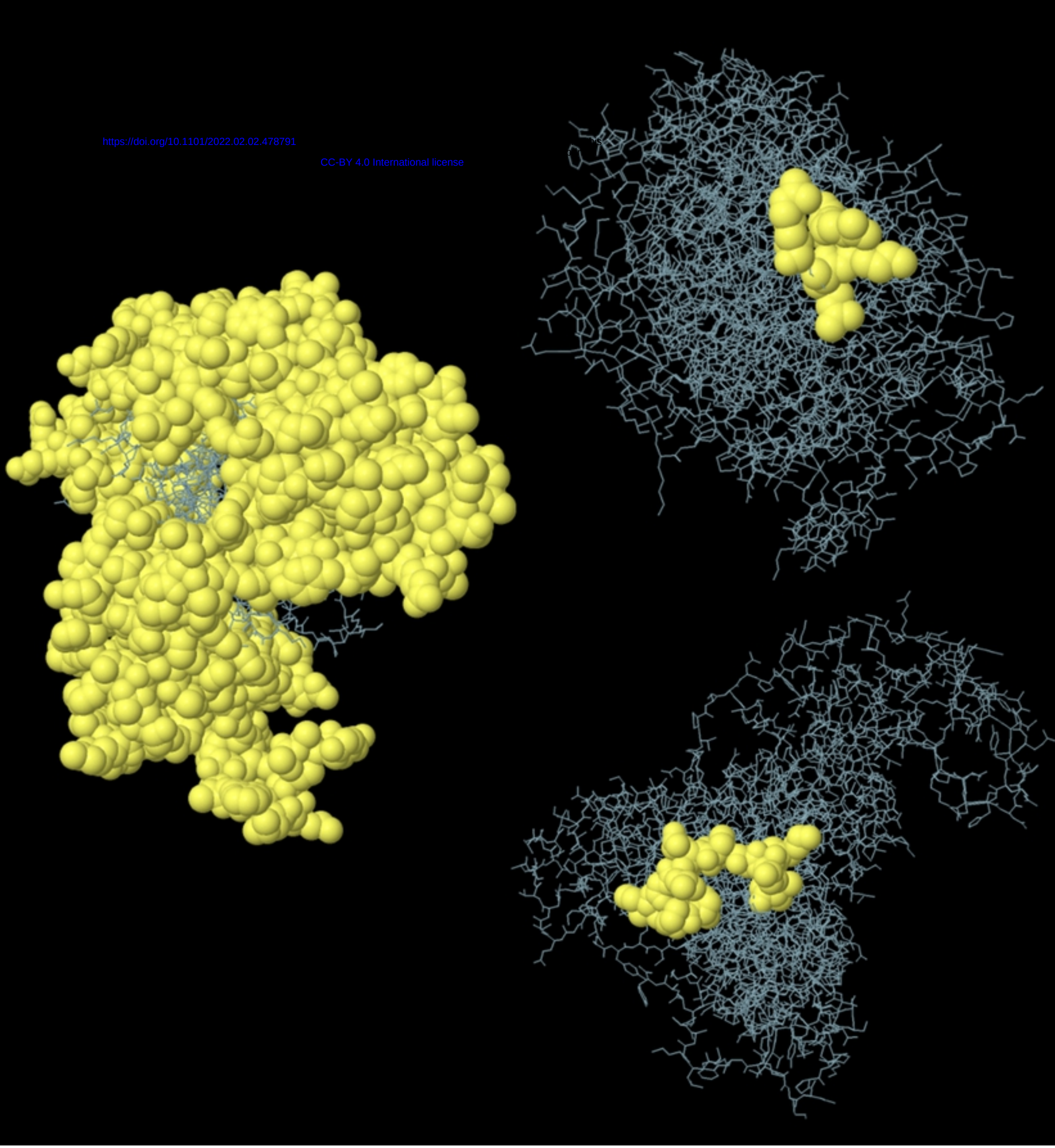

Fig 6

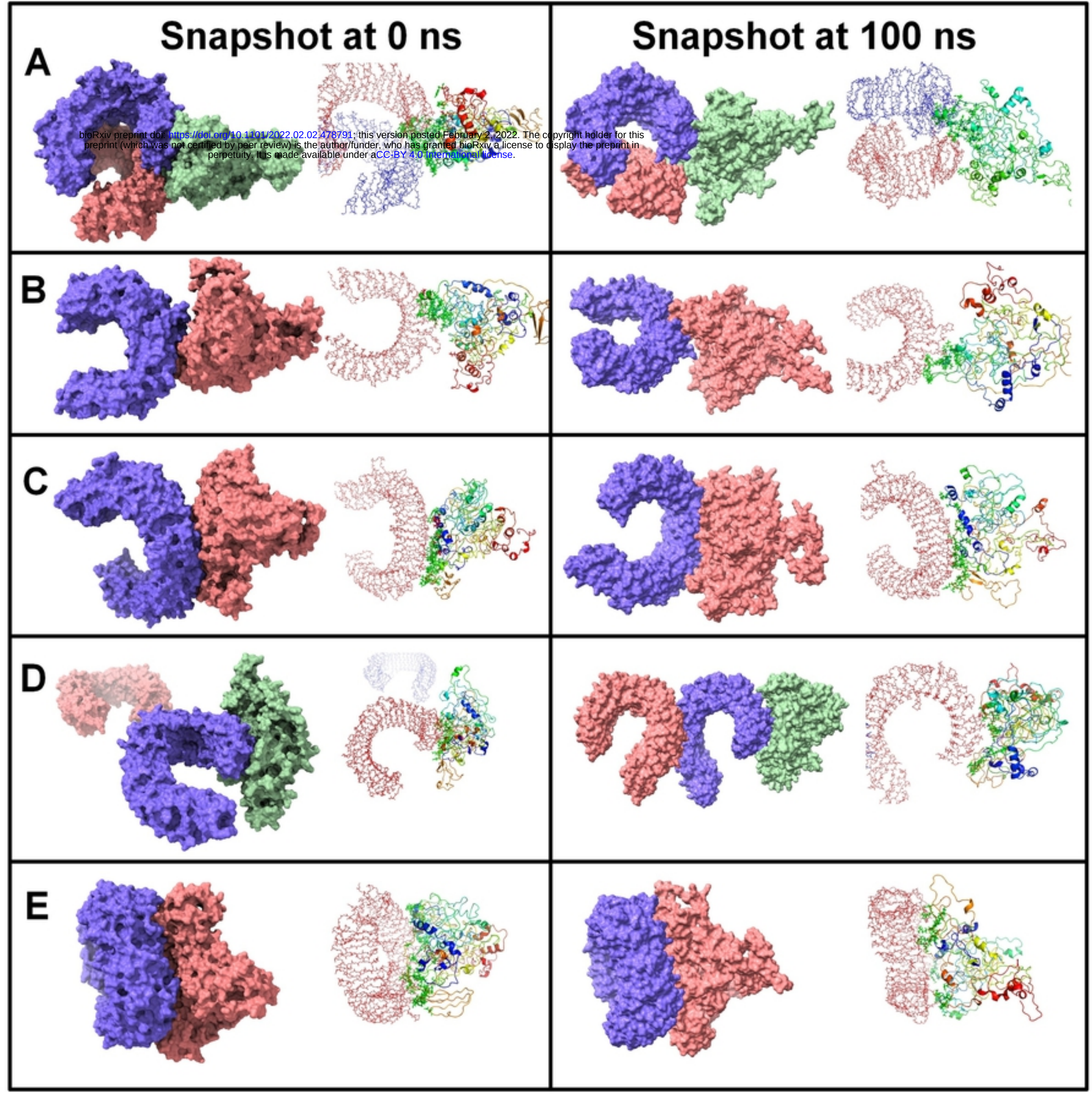

Fig 7

A

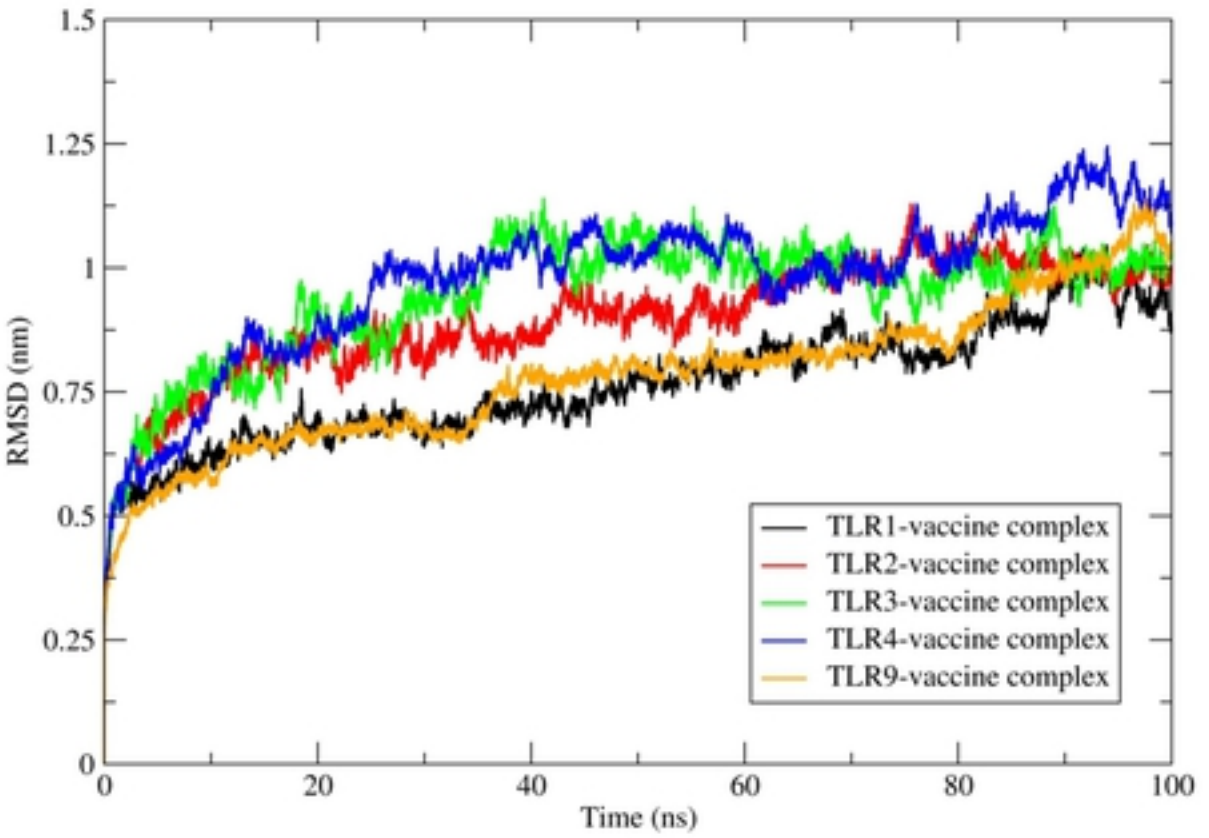
RMSD (nm)
Time (ns)
TLR1-vaccine complex
TLR2-vaccine complex
TLR3-vaccine complex
TLR4-vaccine complex
TLR9-vaccine complex

B

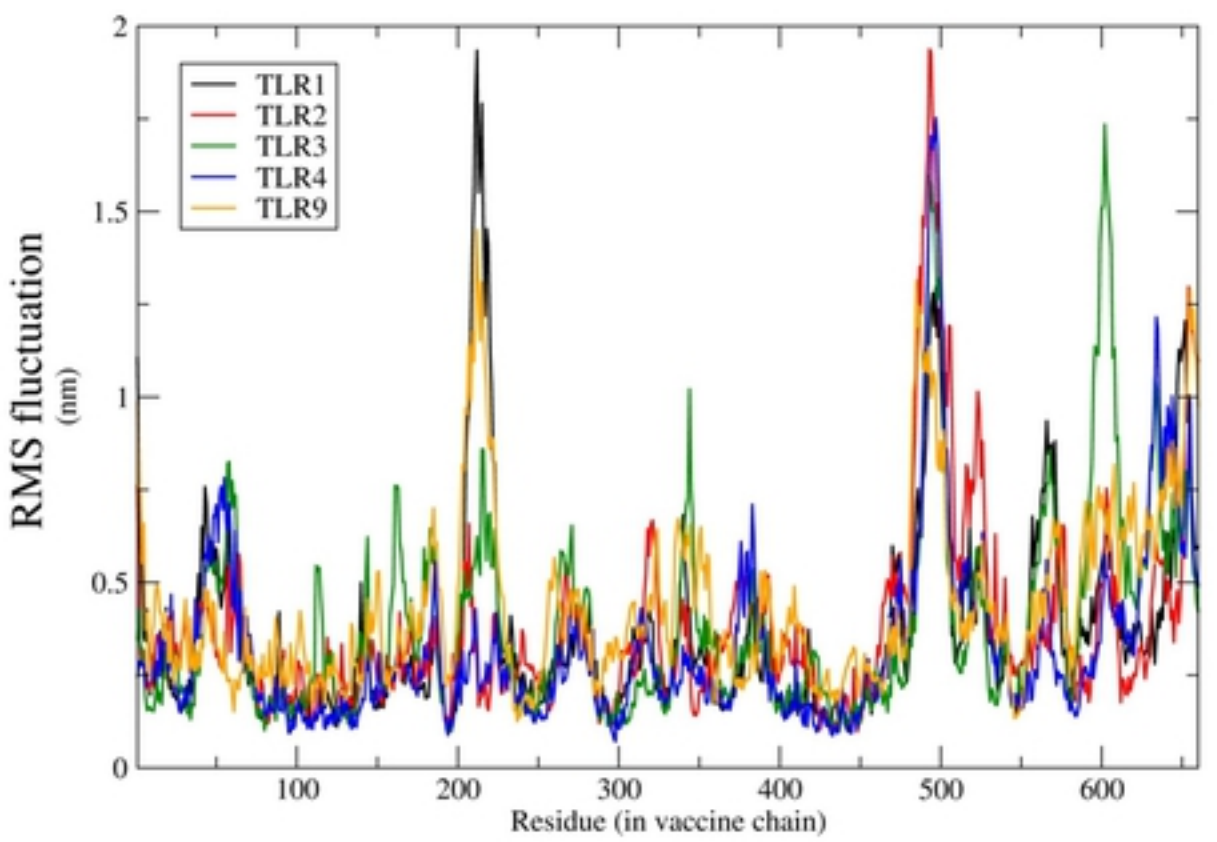
RMS fluctuation (nm)
Residue (in vaccine chain)
TLR1
TLR2
TLR3
TLR4
TLR9

C

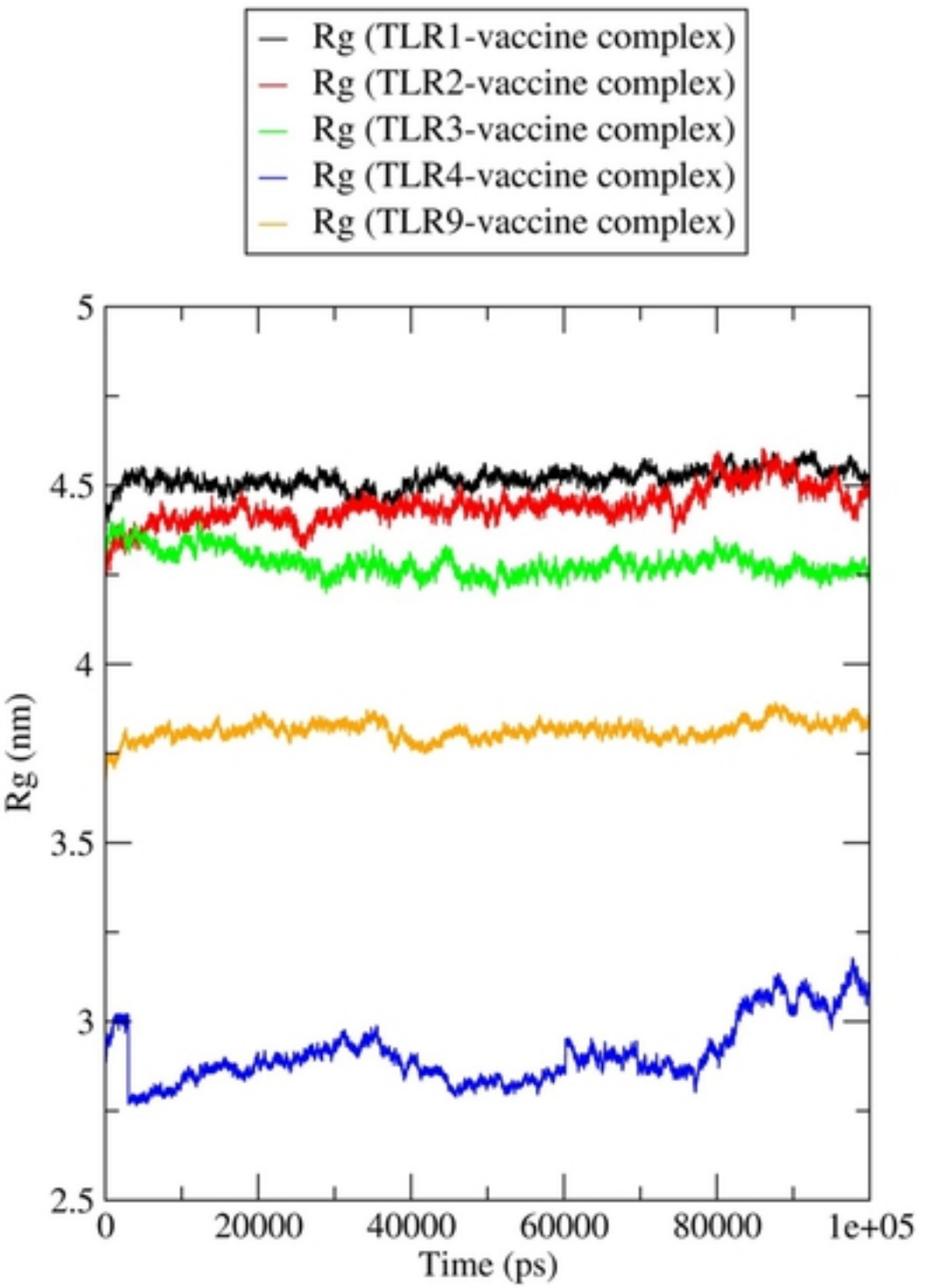
Rg (TLR1-vaccine complex)
Rg (TLR2-vaccine complex)
Rg (TLR3-vaccine complex)
Rg (TLR4-vaccine complex)
Rg (TLR9-vaccine complex)
Rg (nm)
Time (ps)

Fig 8

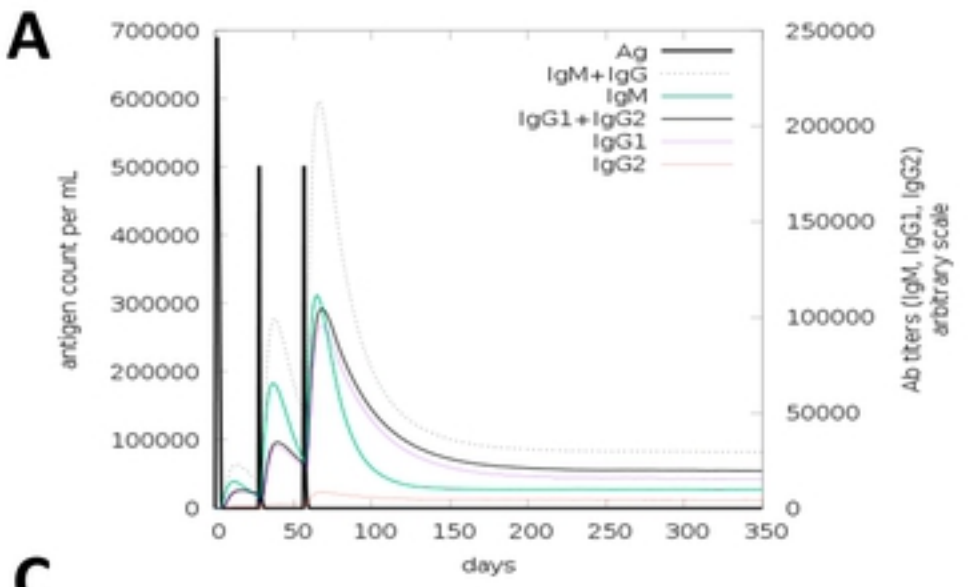

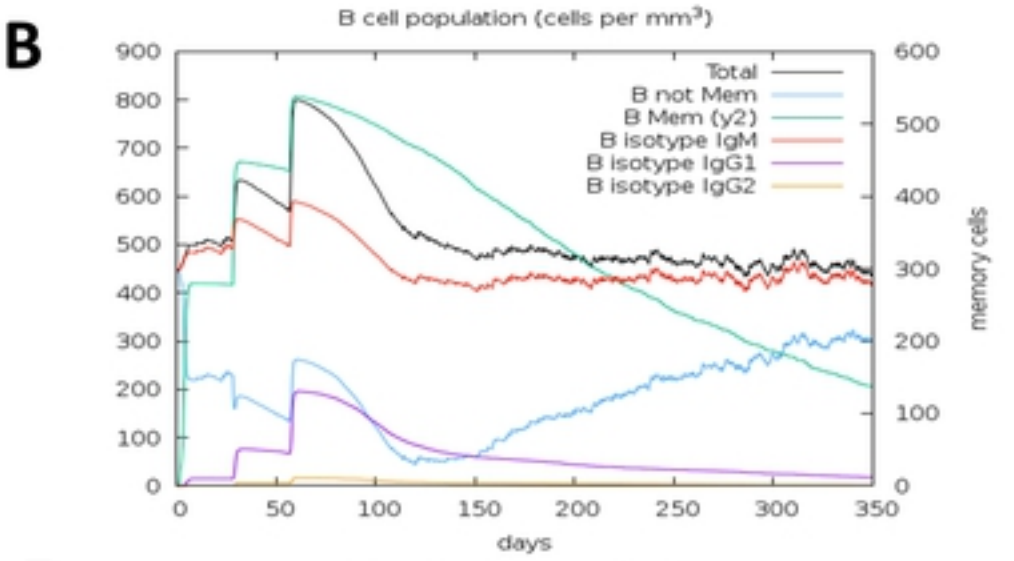

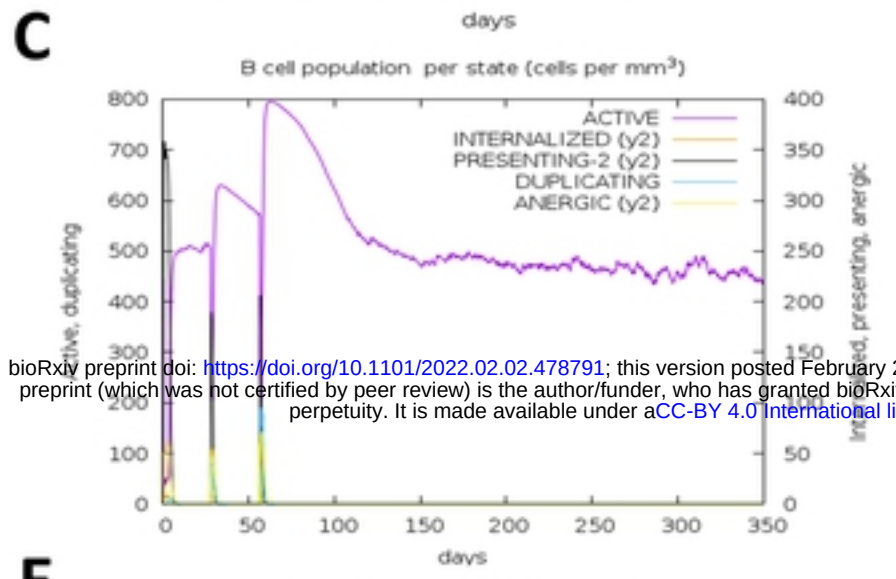

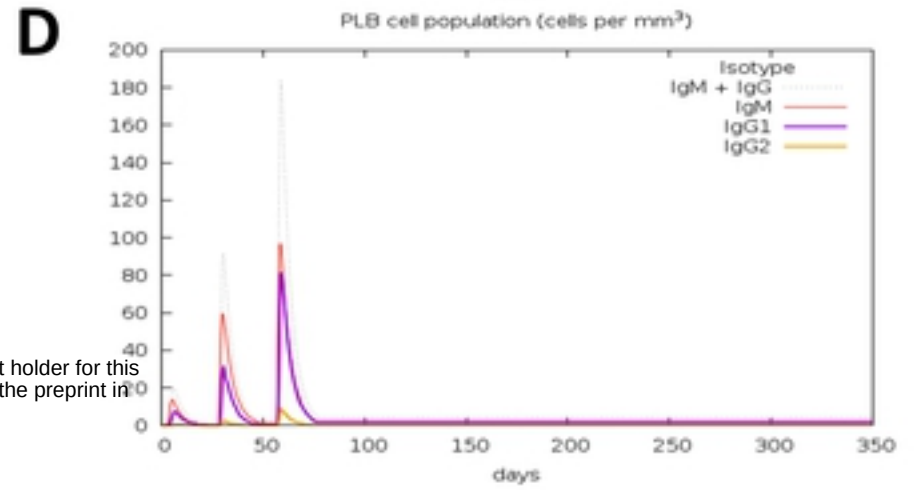

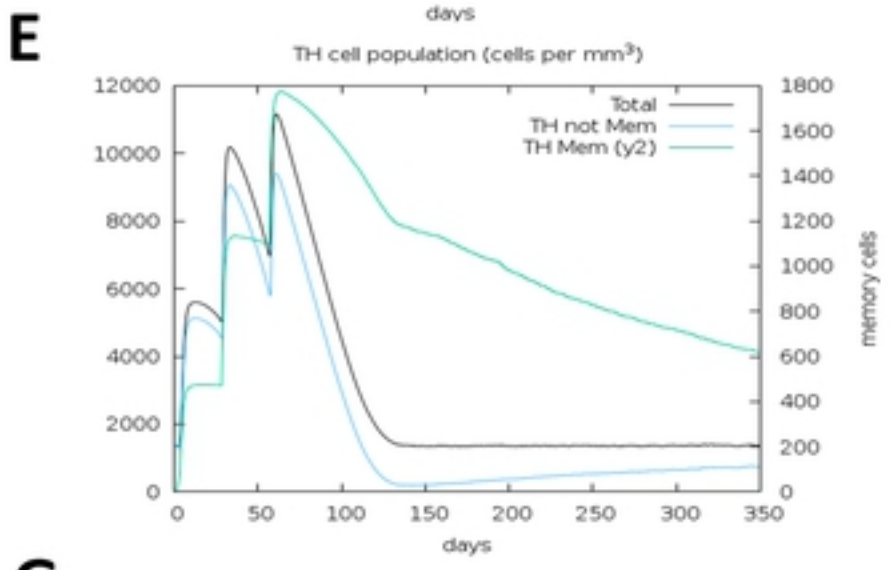

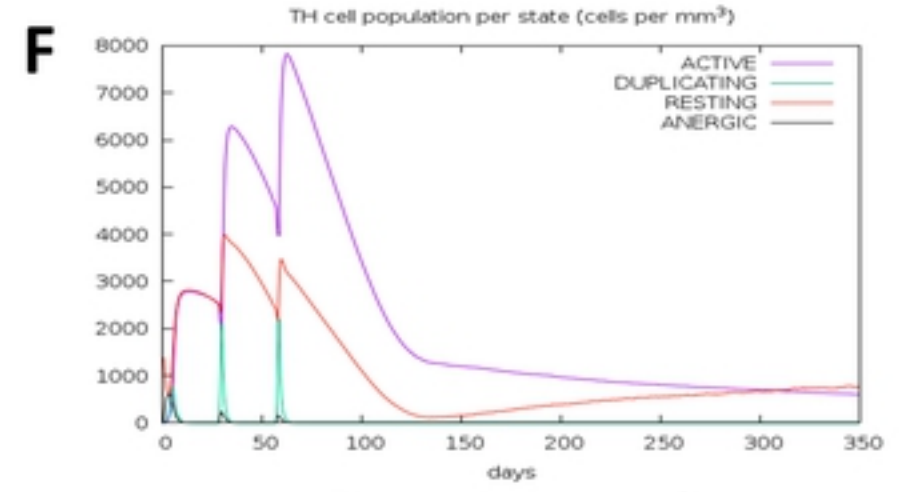

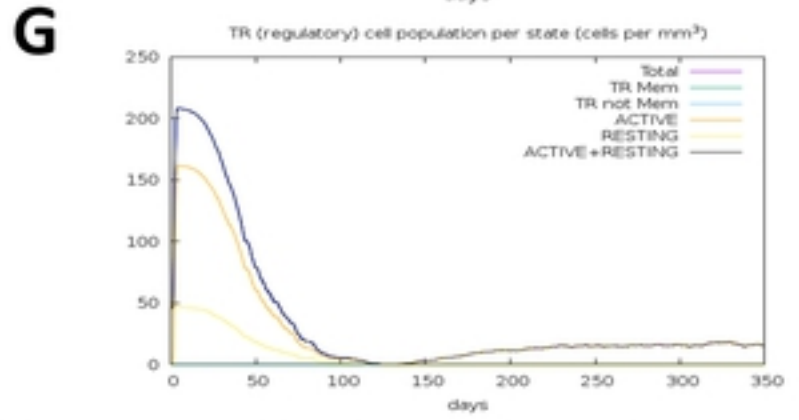

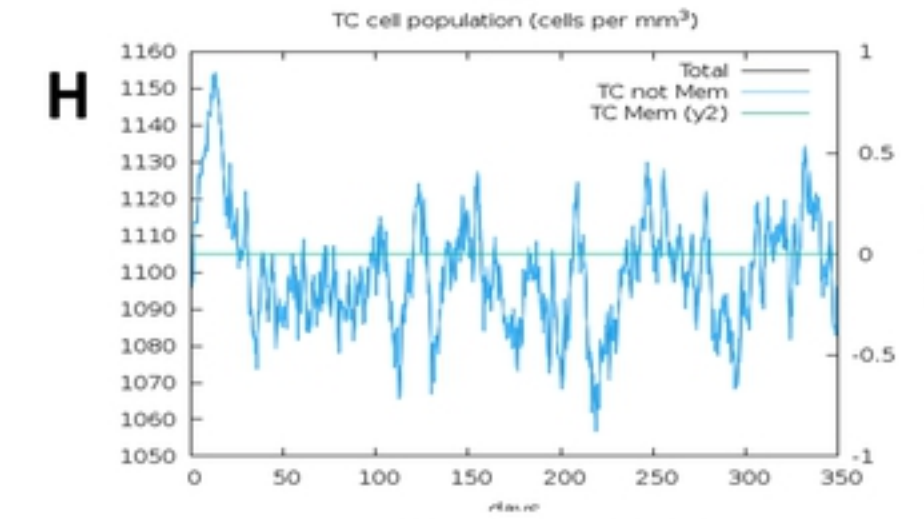

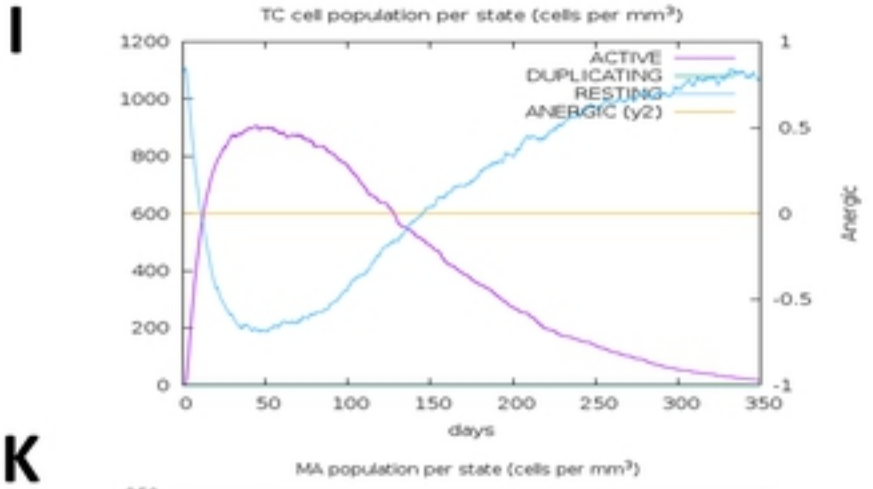

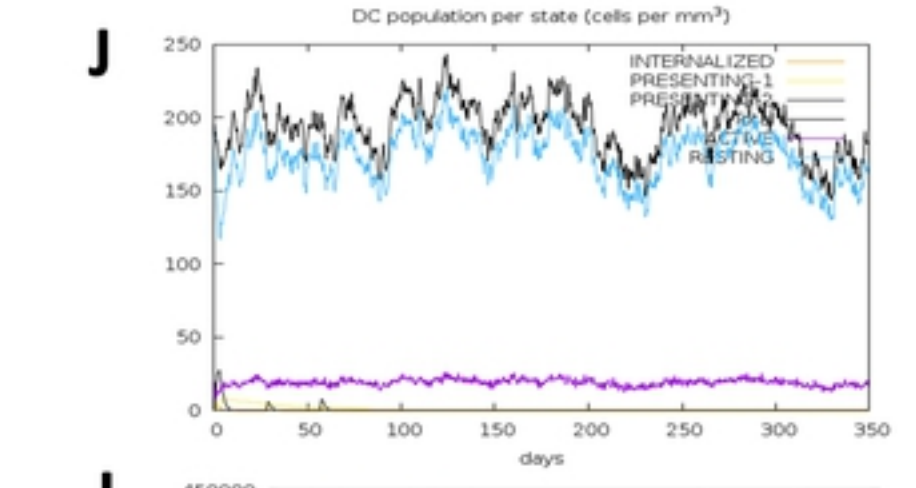

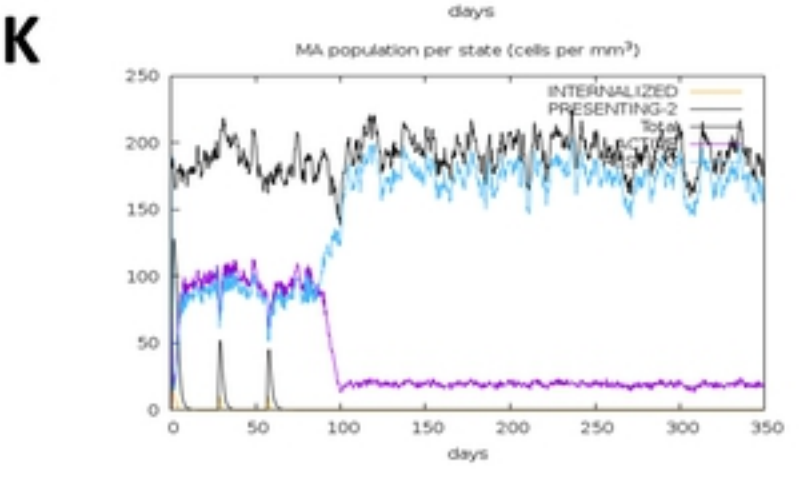

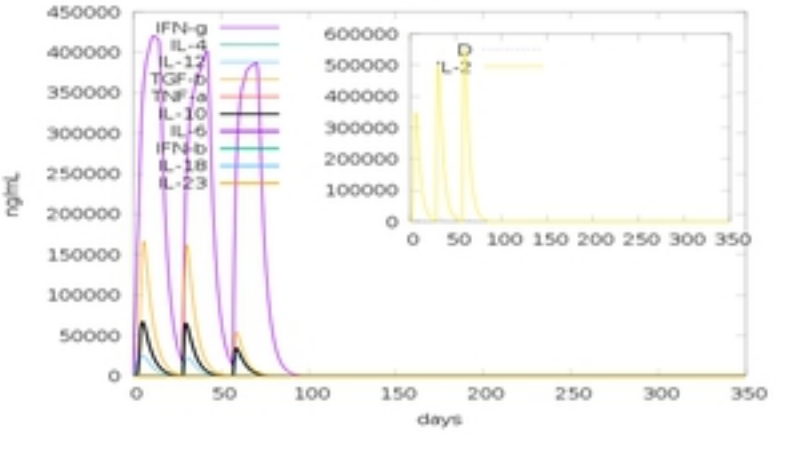

Fig 9